uOttawa

L'Université canadienne
Canada's university

FACULTÉ DES ÉTUDES SUPÉRIEURES ET POSTOCTORALES

uOttawa

L'Université canadienne
Canada's university

FACULTY OF GRADUATE AND POSDOCTORAL STUDIES

Thilina Dewpura

AUTEUR DE LA THÈSE / AUTHOR OF THESIS

M.Sc. (Biochemistry)

GRADE / DEGREE

Department of Biochemistry, Microbiology and Immunology

FACULTÉ, ÉCOLE, DÉPARTEMENT / FACULTY, SCHOOL, DEPARTMENT

Importance of Phosphorylation in PCSK9 Processing, Stability and Function.

TITRE DE LA THÈSE / TITLE OF THESIS

Majambu Mbikay

DIRECTEUR (DIRECTRICE) DE LA THÈSE / THESIS SUPERVISOR

CO-DIRECTEUR (CO-DIRECTRICE) DE LA THÈSE / THESIS CO-SUPERVISOR

Lynn Megeney

Zemin Yao

Gary W. Slater

Le Doyen de la Faculté des études supérieures et postdoctorales / Dean of the Faculty of Graduate and Postdoctoral Studies

IMPORTANCE OF PHOSPHORYLATION IN PCSK9 PROCESSING, STABILITY AND FUNCTION.

By

Thilina Dewpura

Thesis submitted to the Department of Biochemistry, Microbiology and Immunology in partial fulfillment of the requirements for the degree of Master of Science.

Department of Biochemistry, Microbiology and Immunology
Faculty of Medicine
University of Ottawa
Ottawa, Ontario, CANADA
May 2010

Your file Votre référence
ISBN: 978-0-494-69020-8
Our file Notre référence
ISBN: 978-0-494-69020-8

Abstract

Proprotein convertase subtilisin/kexin type 9 (PCSK9) is a secreted glycoprotein regulating the degradation of low density lipoprotein receptor. Single nucleotide polymorphisms in *PCSK9* associate with both hyper- and hypo-cholesterolemia; studies show significant reduction in risk of coronary heart disease for 'loss of function' PCSK9 carriers. We used a combination of mass spectrometry and radiolabeling to report that PCSK9 is phosphorylated at two sites, Ser47 in its propeptide, and Ser688 in its C-terminus. Site directed mutagenesis (SDM) demonstrated that a Golgi casein kinase-like kinase was responsible for PCSK9 phosphorylation based on the consensus site, SXE/S(p). PCSK9 phosphorylation is cell-type specific; phosphorylation status did not affect PCSK9 processing or secretion. Phosphorylated PCSK9 propeptide is protected against proteolysis. Immunoblotting demonstrated that PCSK9 mutants engineered by SDM to prevent phosphorylation at either site (substitution to Ala) or in combination resulted in significantly increased LDLR levels in HuH7 cells by up to ~25%. PCSK9 mutants engineered by SDM to mimick phosphorylation (substitution to Asp/Glu) at the N-terminus, but not at the C-terminus or in combination, promoted LDLR degradation significantly more than wild-type. Far western analysis demonstrated that preventing PCSK9 phosphorylation promoted its interaction with the endogenous inhibitor Annexin A2.

Acknowledgements

I wish to take this opportunity to thank my thesis supervisors Dr. Majambu Mbikay and Dr. Janice Mayne for their wisdom and guidance. Special thanks to all the research support staff including technicians Angela Raymond, Francine Sirois and administrative assistant JoAnn McDonald. Canadian Institutes of Health Research (CIHR) is acknowledged for their support of this research project through a grant to my supervisors Drs. Mbikay and Mayne, which supplied my graduate stipend.

Table of Contents

List of Tables

List of Figures

List of Abbreviations

Ab: Antibody

ADH: Autosomal Dominant Hypercholesterolemia

Apo-B100: Apolipoprotein B100

CDCA: Chenodeoxycholic Acid

CHO K1: Chinese Hamster Ovarian K1

CHRD: Cys/His-rich Domain

CKII: Casein Kinase II

DMEM: Dulbecco's Modified Eagle's Medium

EGF-A: Epidermal Growth Factor-like repeat domain A

ER: Endoplasmic Reticulum

FH: Familial Hypercholesterolemia

FXR: Farnesoid X Receptor

GCK: Golgi Casein Kinase

HNF1α: Hepatocyte Nuclear Factor

HEK 293: Human Embryonic Kidney

IGFBPs: Insulin-like Growth Factor Binding Proteins

KO: Knock-out

LDLC: Low Density Lipoprotein Cholesterol

LDLR: Low Density Lipoprotein Receptor

MS: Mass Spectrometry

NF-Y: Nuclear Factor-Y element

PCSK: Proprotein convertase subtilisin/kexin

PCSK9: Proprotein convertase subtilisin/kexin type 9

PTM: Post-translational Modification

SAP: Shrimp Alkaline Phosphatase

^{35}S Cys/Met : ^{35}S Cysteine/Methionine

SDM: Site Directed Mutagenesis

SDS-PAGE: Sodium Dodecyl Sulfate Polyacrylamide Gel Electrophoresis

si-RNA: small interfering RNA

SNP: Single Nucleotide Polymorphism

SO_4^{2-}-propeptide: Sulfated PCSK9 propeptide

SO_4^{2-}/ PO_4^{2-}-propeptide: (sulfated and phosphorylated) PCSK9 propeptide

Sp-1: Specificity factor-1

SRE: sterol regulatory element

SREBP: Sterol Regulatory Element Binding Protein

TOF-MS: Time of Flight Mass Spectrometry

WT: Wild-type

1. Introduction

1.1 Proprotein Convertase Subtilisin/Kexin Types (PCSKs)

1.1.1 Proprotein Theory

The discovery of the mammalian proprotein convertase subtilisin/kexin-like (PCSKs) family in the late 1980's and early 1990's was the culmination of separate studies that had begun over two decades earlier to identify the endoproteases involved in the *in vivo* proteolytic maturation of various precursor substrates found in the secretory pathway to biologically active compounds. This stemmed from a hypothesis proposed separately by two groups that peptide hormones were derived intracellularly from higher molecular weight precursors through post-translational endoproteolysis. In the late 1960s, Donald Steiner and colleagues used pulse-chase labeling and isolated a protein of higher molecular weight than insulin, which upon treatment with trypsin was cleaved to a form that was indistinguishable from insulin [1]. This larger protein was later confirmed to be the precursor form of insulin, which they named proinsulin, coining the first moniker for a precursor protein [2]. Separately - Michel Chrétien and colleagues showed that β-melanocyte stimulating hormone was found within the larger β- and γ lipotrophic hormone using chemical sequencing techniques [3].

By the late 1980s, with developing DNA sequencing and cloning techniques, studies conducted in the yeast *Saccharomyces cerevisiae* by Julius and colleagues identified the prototypical eukaryote convertase, the serine protease yeast kexin, which was similar to the bacterial prototype subtilisin, and capable of cleaving α-mating factor at various dibasic sites through endoproteolysis [4]. These observations substantiated the idea that some functional

peptides could exist within inactive protein precursors (proproteins) that could be converted into an array of biologically active molecules, introducing another level of protein diversity. Genes homologous to yeast kexin were later identified, leading to discoveries of the nine known mammalian homologues beginning with the mammalian prototype PCSK3/Furin, up to the most recently discovered proprotein convertase subtilisin/kexin-like 9 (PCSK9) [5-19].

1.1.2 Proprotein Convertase Subtilisin/Kexin Domain Structure and Function

The serine protease family of mammalian PCSKs consists of nine members, seven of which (PCSKs1-7) are closely related to yeast kexin, and two others (PCSKs 8 and -9) closely related to pyrolysin and proteinase K, respectively (Figure 1) [5-16, 18-21]. Collectively, the PCSKs are involved in the proteolytic maturation of various substrates into biologically active molecules including proneuropeptides, prohormones, proreceptors, growth factors, cell surface proteins and serum proteins [22-27].

Sharing similar structural homology, the multi-domain PCSKs consist of a signal peptide, a prodomain, catalytic domain, a P-domain, and a C-terminal domain (Figure 1) [28, 29]. The signal peptide directs nascent proteins to the endoplasmic reticulum (ER) for maturation through the secretory pathway. The prodomain functions as both an endogenous inhibitor and as an intramolecular chaperone, assisting in nascent protein folding (Figure 1) [29]. The prodomain is autocatalytically cleaved early in endoplasmic reticulum (ER) to form a heterodimer between the propeptide and the rest of the molecule, and this interaction is required for transit out of the ER and to the Golgi apparatus [30]. As the PCSK

Figure 1. Schematic of Proprotein Convertase Subtilisin/Kexin (PCSK) Family. The serine protease family of mammalian PCSKs consists of nine members, seven of which (PCSKs1-7) are closely related to yeast kexin, and two others (PCSKs 8 and -9) closely related to pyrolysin and proteinase K, respectively. The PCSKs share similar structural homology; shown are the signal peptide domain that directs the PCSK to the ER; prodomain which acts as an endogenous inhibitor and intermolecular chaperone to assist in proper protein folding; the highly conserved catalytic domain; a P-domain which determines optimal pH for PCSK activity; and the variable C-terminal domain which is involved in protein-protein interactions. PCSK3/Furin, PCSK5B, PCSK6, PCSK7 and PCSK8 additionally possess a transmembrane domain and cytoplasmic domain.

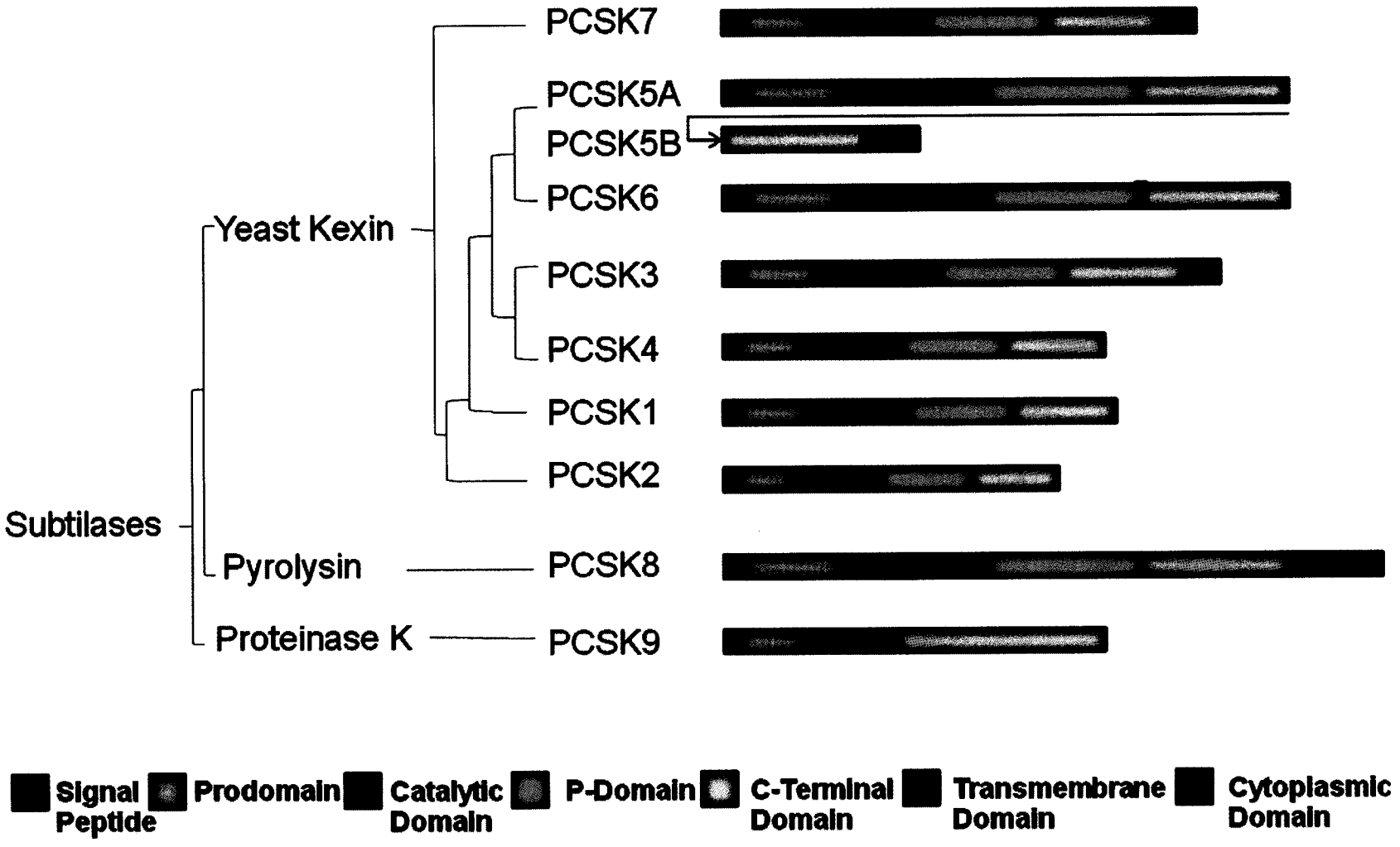
PCSK7
PCSK5A
PCSK5B
PCSK6
Yeast Kexin
PCSK3
PCSK4
PCSK1
PCSK2
Subtilases
Pyrolysin
PCSK8
Proteinase K
PCSK9
Signal Peptide
Prodomain
Catalytic Domain
P-Domain
C-Terminal Domain
Transmembrane Domain
Cytoplasmic Domain

travels from the Golgi apparatus and secretory vesicles, a second proteolytic cleavage event occurs within the inhibitory propeptide that releases it from the mature PCSK, activating the enzymatic property of the PCSK [31]. The only exception is the propeptide of PCSK9 which does not undergo this secondary cleavage, and remains in tight association with PCSK9 [12]. The catalytic domain is a highly conserved domain throughout the convertase family, with critical residues histidine, aspartic acid, and serine forming the 'catalytic triad' typical of serine proteases, and an asparagine at the oxyanion hole [29]. PCSKs1-7 recognize substrates with dibasic cleavage motifs ((K,R)-X_n-(K,R)↓, where X is any amino acid, n=0,2,4,6 and ↓ represents cleavage), while PCSK8 recognizes a hydrophobic (R,K)-X-hydrophobic-(L,T,K,F)↓ and PCSK9 an acidic VFAQ↓ motif (Figure 1) (Table 1) [12, 21, 31-34]. The P-domain provides stability to the convertase, determines functional pH optimum of the enzyme and functions as an intramolecular chaperone as well (Figure 1) [29, 35]. The C-terminal domain is the most variable domain of this family and is also involved with maintaining protein stability, intermolecular protein-protein interactions as well as trafficking (Figure 1) [31]. In addition PCSK3/Furin, PCSK5B, PCSK6, PCSK7 and PCSK8 possess a transmembrane domain (Figure 1) [18, 19, 33, 36, 37].

1.1.3 PCSK Subcellular Localization, Tissue Distribution, and Physiology

Substrate specificity of a given PCSK is shaped not only by its consensus cleavage motif (Table 1) but also by parameters including subcellular localization and tissue distribution. The ability of a PCSK to cleave a potential substrate, one which contains its consensus motif, depends on both the PCSK and substrate being not only expressed in the same tissue, but

Table 1. Nomenclature, Subcellular Colocalization and Tissue Distribution of the PCSKs

Current Nomenclature	Old Nomenclature	Cleavage Motif	Subcellular Colocalization	Tissue Distribution	Substrate (example)	Knockout Phenotype
PCSK1	PC1/PC3	(R/L)-X_n-R↓	SG	Neuronal, Enteroendocrine	proinsulin	Obesity/ Diabetes
PCSK2	PC2	(R/L)-X_n-R↓	SG	Neuronal, Enteroendocrine	proglucagon	Lean /resistant to diet induced obesity
PCSK3	PC1/PACE/ Furin	(R/L)-X_n-R↓	TGN, PM	Ubiquitous	Von Willebrand Factor	Embryonic lethal
PCSK4	PC4	(R/L)-X_n-R↓	TGN, PM	Gonad	Insulin Growth Factor	Infertile
PCSK5A **PCSK5B**	PC5/6	(R/L)-X_n-R↓	SG TGN, PM	Widespread Widespread		Embryonic lethal
PCSK6	PACE4	(R/L)-X_n-R↓	TGN, PM	Ubiquitous	Bone Morphogenic Protein	25% Embryonic lethal
PCSK7	LPC/SPC7/PC7	(R/L)-X_n-R↓	TGN, PM	Ubiquitous	Platelet-derived growth factor	No Observed phenotype
PCSK8	SKI-1, Site-1 Protease (S1P)	R/K-X-(L,I,V)-Z↓	TGN, PM	Ubiquitous	SREBP-1a, -1c, -2	Embryonic lethal
PCSK9	NARC-1	VFAQ↓SIP	Secreted	Liver, Intestine	N/A	Enhanced LDLc clearance

n=0, 2, 4, or 6; X= any amino acid; Z=any amino acid except P, C, E, or V; SG-Secretory Granules; TGN- *trans*-Golgi Network; PM- Plasma Membrane

present in the same subcellular compartment [38, 39]. The expression, distribution, and some well characterized substrates of each PCSK are shown in Table 1.

Much of what we have learned about the physiology and pathophysiology of PCSKs has come from studies of PCSK-null or PCSK knock-out (KO) mouse models and is exemplified by their phenotypes (Table 1) or lack thereof [16, 40-47]. For instance, while PCSK3 is important for development and its KO is embryonically lethal, PCSK7 KO mice show no phenotype, presumably due to redundancy of some PCSKs who share common substrates (Table 1) [16, 42, 48].

The most recently identified members of the PCSK family, PCSK8 and PCSK9, have been shown to play important roles in cholesterol homeostasis. PCSK8 was the first mammalian convertase identified to cleave after non-basic residues [19]. PCSK8 is widely expressed and has a role in the processing of the transcription factors sterol regulatory element-binding proteins (SREBPs) important in cholesterol homeostasis [19]. PCSK8 KO mice are embryonically lethal, and liver-specific conditional knockout mice have disrupted cholesterol and fatty acid synthesis (Table 1) [19, 46].

PCSK9, the most recently discovered convertase family member, is primarily expressed in the liver and intestine, and is constitutively secreted (Table 1) [12]. Aside from its own autocatalytic cleavage, no other substrates are known for PCSK9 [12, 32]. Overexpression and knock-out studies in mice have demonstrated that PCSK9 leads to the post-translational degradation of low density lipoprotein receptors (LDLR) [32, 47, 49, 50]. Therefore, 'loss of function' of PCSK9 leads to reduced plasma low density lipoprotein cholesterol (LDLC)

levels [51, 52]. In fact two healthy 'PCSK9-null' individuals were identified with no circulating PCSK9 levels which has made PCSK9 a very popular topic of study as a viable drug target [53, 54]. Understanding the post-translational regulation of PCSK9, its affect on PCSK9 mediated LDLR degradation and consequently its role in cholesterol homeostasis was the focus of my Masters thesis. The current state of knowledge in this area will be discussed in the following sections.

1.2 Proprotein Convertase Subtilisin/Kexin 9 (PCSK9)

1.2.1 Cholesterol Homeostasis and Modulation by Proprotein Convertase Subtilisin/Kexin 9

The key mediator of cellular cholesterol clearance is the LDLR [55, 56]. This transmembrane glycoprotein found at the cell surface is responsible for binding extracellular LDLC, the major carrier of plasma cholesterol, leading to its endocytosis and metabolism [56, 57]. The extracellular LDL binding repeat domain of LDLR binds the protein component of LDLC, Apolipoprotein B100 (ApoB100) [56, 58]. For the LDLR: LDLC complex to be endocytosed, the cytoplasmic domain of LDLR must bind the autosomal recessive hypercholesterolemia (ARH) adapter protein found on the cytosolic surface of the plasma membrane [59-61]. In the endosomal compartment, the decreasing pH causes the LDL binding repeat domain of LDLR to fold in towards its epidermal growth factor-like motif, forming a hairpin structure allowing LDLC to dissociate from LDLR [62, 63]. While the LDLR is recycled back to the plasma membrane in a recycling endosome, LDLC translocates to late endosomes for degradation in the lysosome (Figure 2) [56].

Figure 2. Cholesterol Uptake Pathway and PCSK9 Mechanism of Action. (*Right side*) In the absence of PCSK9, the ligand binding domain of LDLR binds to extracellular LDL-C, and this complex is endocytosed. In an endosomal compartment, LDL-C dissociates from LDLR, LDL-C translocates to the lysosome to be metabolized, while LDLR is recycled to the plasma membrane. (*Left side*) In the presence of PCSK9, PCSK9 binds to LDLR at its EGF-A domain. This complex is endocytosed, and at the lower environmental pH of late endosomal compartments, PCSK9 remains tightly bound to LDLR. This complex translocates to the lysosome for degradation.

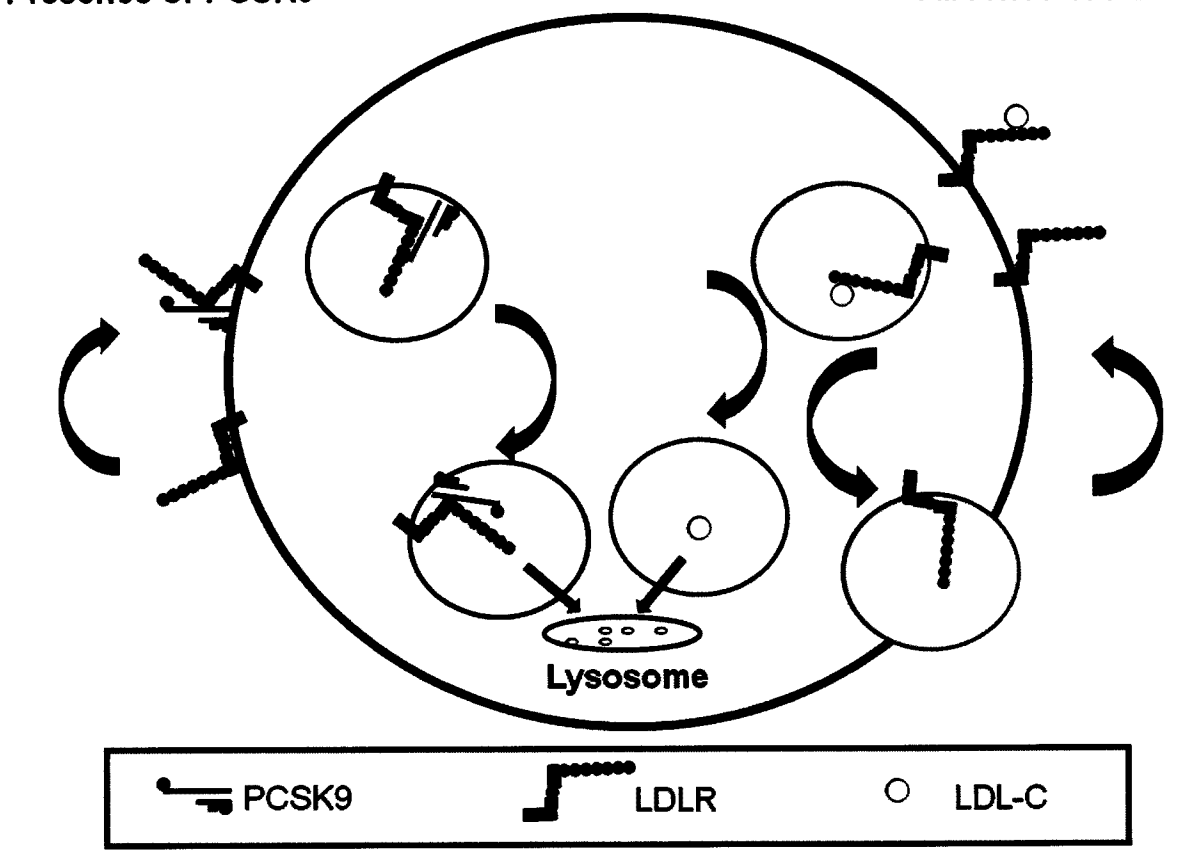
Presence of PCSK9
Absence of PCSK9
Lysosome
PCSK9
LDLR
LDL-C

Familial hypercholesterolemia (FH) is an autosomal dominant disease causing increased serum cholesterol levels, plaque formation, xanthomas, premature atherosclerosis and increased risk of myocardial infarction [64, 65]. Three genetic loci have been identified as causes of familial hypercholesterolemia including *LDLR*, *ApoB100* and *PCSK9* (known as FHs1-3, respectively) [66-69]. In the mid-1970s, metabolic labeling studies conducted by Joseph Goldstein, Michael Brown and colleagues led to the identification of the first heritable factor of this disorder – LDLR [67]. Impairment of this receptor in patients heterozygous or homozygous for FH1 results in decreased biosyntheses, binding or internalization of LDLC [70, 71]. By 1984 the gene encoding human LDLR was mapped to chromosome 19, the same locus that the gene responsible for FH1 had been mapped to in pedigree studies [72], and with the advent of cloning and sequencing techniques, many human mutations inactivating LDLR and causing FH1 have since been identified [73].

Shortly after the identification of mutations in *LDLR* as a cause of autosomal dominant hypercholesterolemia (ADH), cases of hypercholesterolemic patients were discovered where LDLR levels were unaffected [69, 74]. In some of these patients, mutations were identified in the binding site of the protein component of the LDL ligand, ApoB100, resulting in defective receptor binding, and reduced efficiency of LDL clearance leading to a hypercholesterolemic phenotype [68]. Thus 'loss of function' mutations of ApoB100 were associated with a second form of familial hypercholesterolemia (FH2), further demonstrating the genetic heterogeneity of hypercholesterolemia [68, 69].

By the early twenty-first century, mutations in LDLR and ApoB accounted for many but not

Figure 3. Schematic of *PCSK9* Single Nucleotide Polymorphisms Affecting Plasma LDL-C Levels. Schematic of PCSK9 exons depicting several sites of single nucleotide polymorphisms, that have been identified to associate with either hypercholesterolemia (red), or hypocholesterolemia (blue). SNPs associated with mild hyper- or hypocholesterolemia, or that have no known effect are presented in grey panels.

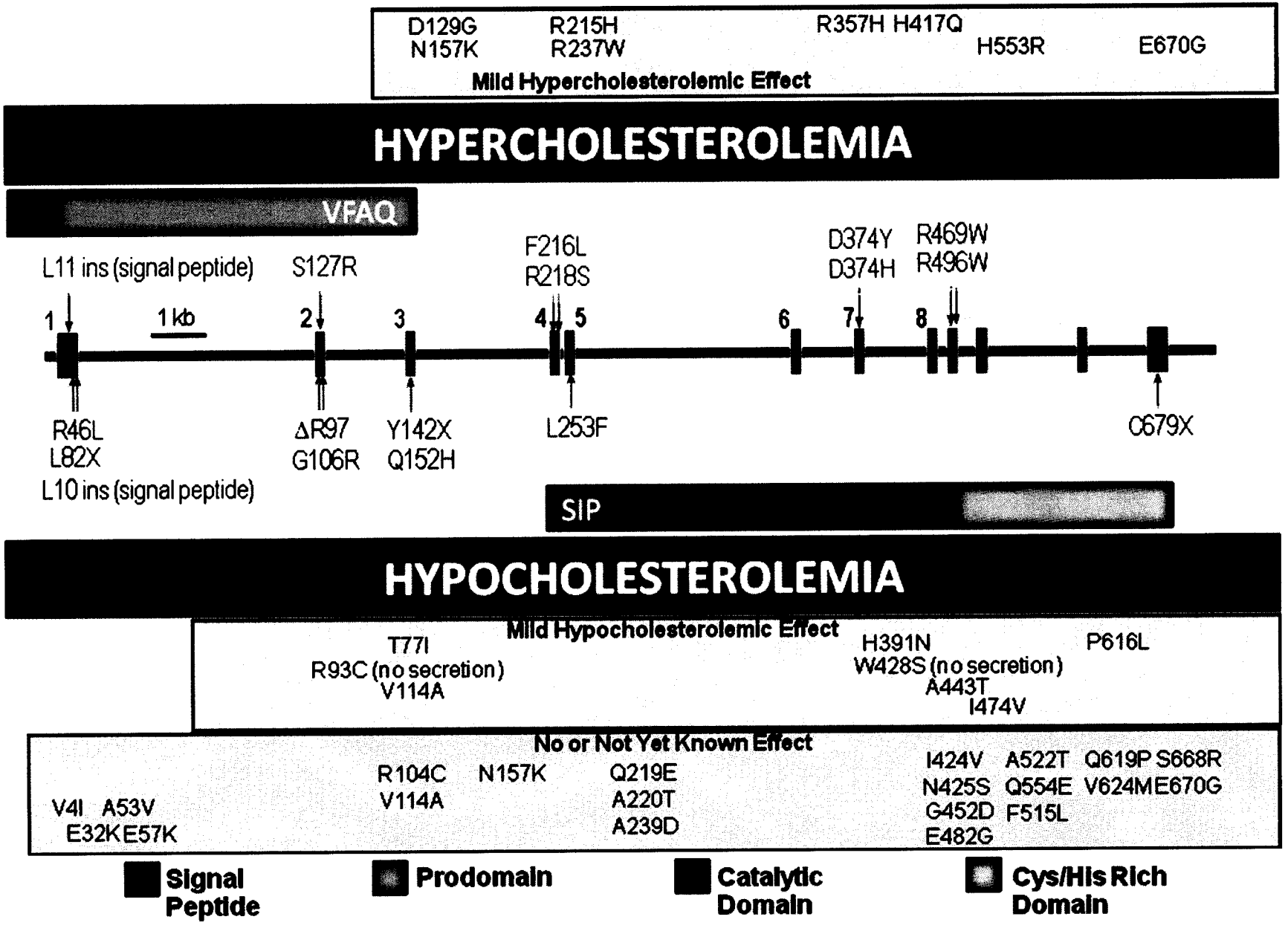
D129G
N157K
R215H
R237W
R357H H417Q
H553R
E670G
Mild Hypercholesterolemic Effect
HYPERCHOLESTEROLEMIA
VFAQ
L11 ins (signal peptide)
S127R
F216L
R218S
D374Y
D374H
R469W
R496W
1
1 kb
2
3
4
5
6
7
8
R46L
L82X
L10 ins (signal peptide)
ΔR97
G106R
Y142X
Q152H
L253F
C679X
SIP
HYPOCHOLESTEROLEMIA
Mild Hypocholesterolemic Effect
T77I
R93C (no secretion)
V114A
H391N
W428S (no secretion)
A443T
I474V
P616L
No or Not Yet Known Effect
V4I
A53V
E32K
E57K
R104C
V114A
N157K
Q219E
A220T
A239D
I424V
N425S
G452D
E482G
A522T
Q554E
F515L
Q619P
V624M
S668R
E670G
Signal Peptide
Prodomain
Catalytic Domain
Cys/His Rich Domain

all cases (~81% collectively) of FH, prompting groups to search for other causal genes [28, 75]. In 2003, Abifadel and colleagues reported several cases of FH within two French families and who did not carry mutations in either the *LDLR* or *ApoB* genes [66]. Instead two dominantly segregating missense mutations were identified in a third gene, encoding the newly identified proprotein convertase, PCSK9, which resulted in an amino acid substitution of S127R in its prodomain and F216L in its catalytic domain, that associated with hypercholesterolemia (FH3) (Figure 3) [66]. The following year, a third mutation in the catalytic domain of PCSK9 at D374Y was identified in a Utah kindred and associated with a hypercholesterolemic phenotype similar in severity to LDLR mutations (Figure 3) [76]. *PCSK9* is a highly polymorphic gene, with over 50 single nucleotide polymorphisms (SNPs) having been identified over the past several years, associating with variable levels of plasma LDLC profiles in human populations (Figure 3) [51, 52, 64, 66, 77, 78]. 'Gain-of-function' mutations in PCSK9 describe 2.3% of hypercholesterolemia [28]. Other heritable factors associating with hypercholesterolemia have yet to be identified.

In 2005, Cohen and colleagues sought to identify mutations in *PCSK9* which could cause an opposite phenotype to hypercholesterolemia [51]. In the Dallas Heart Study, three such "loss-of-function" mutations were identified in the population with the lowest plasma LDLC levels ($<5^{th}$ percentile) and associating with hypocholesterolemia; the PCSK9 nonsense mutations PCSK9(C679X) and PCSK9(Y142X), found in African-Americans and the missense mutation PCSK9(R46L) found in Caucasians (Figure 3) [51]. Individuals with any of these mutations had greatly reduced plasma LDLC levels (21% with PCSK9(R46L) mutation and 40% with PCSK9(Y142X)/ PCSK9(C679X) mutations) [51, 52]. In longitudinal population studies, individuals with these mutations were protected from

cardiovascular disease (47% with PCSK9(R46L) mutation and up to 88% with PCSK9(C679X) mutation) [52]. Our group has recently identified a novel mutation at the PCSK9 autocatalytic cleavage site, in a French-Canadian population which is associated with a 68% reduction in plasma LDLC levels, and that in cell culture prevents autocatalytic cleavage and subsequent secretion of PCSK9 (Mayne *et al.* 2010 (manuscript in progress), Figure 3).

1.2.2 PCSK9 Expression and Transcriptional Regulation

PCSK9 is a 12 exon gene found on chromosome 1 (1p32) encoding a 692 amino acid (aa) preproprotein [12]. PCSK9 mRNA is highly expressed in the liver and intestine, two tissues important in cholesterol homeostasis (Table 1) [12]. Several regulatory elements have been identified in the proximal promoter of PCSK9 including nuclear factor-Y element (NF-Y), specificity factor-1 (Sp-1), sterol regulatory element (SRE), E-box, and hepatocyte nuclear factor (HNF1α) binding site (Figure 4) [49, 79-81]. Early microarray studies by Park and colleagues demonstrated that *PCSK9* was negatively regulated by intracellular cholesterol status through the SRE in its proximal promoter that recognizes the transcription factor sterol regulatory element binding protein-2 (SREBP-2) [49]. This transcription factor is part of a family that includes SREBPs -1a, -1c, and -2 which activate genes involved in fatty acid synthesis and cholesterol biosynthesis, including LDLR [82-85]. We, and others, have shown HMG-CoA reductase inhibitors (statins), which block the rate-limiting step in intracellular cholesterol biosynthesis and activate the SREBP pathway, upregulate PCSK9 and LDLR expression [80, 86].

Figure 4. *PCSK9* Gene Schematic. *PCSK9* gene schematic depicting its 12 exons in relation to PCSK9 signal peptide (red), prodomain (blue), catalytic domain (brown), or C-terminal domain (yellow). Several regulatory elements are found within the PCSK9 proximal promoter including: Nuclear Factor-Y element (-613bp), Specificity Factor-1 (Sp1, -430bp and -198bp), sterol regulatory element (SRE, -355 to -333bp), Hepatocyte Nuclear Factor 1α (HNF1α) binding site (-386 to -374bp), and an E-box (-1277 to -1261bp).

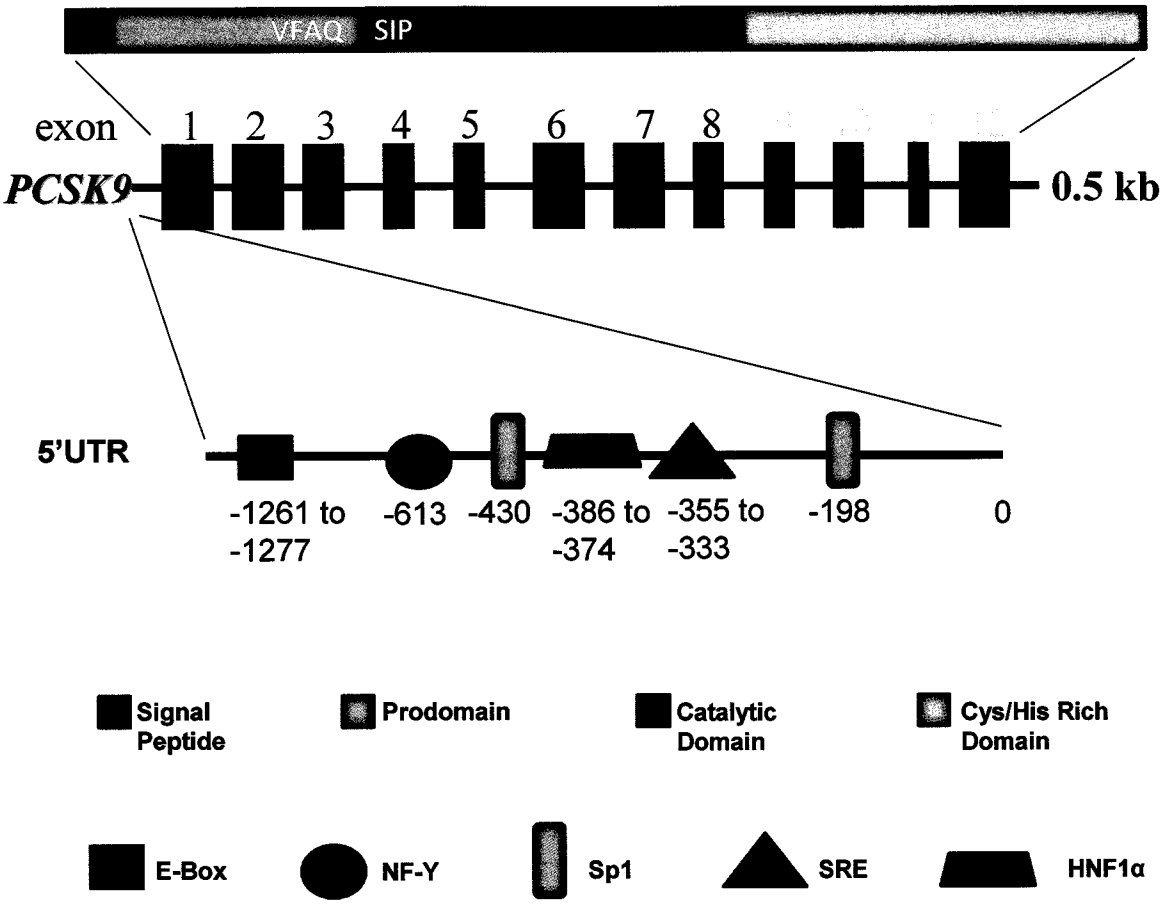
VFAQ
SIP
exon
1
2
3
4
5
6
7
8
PCSK9
0.5 kb
5'UTR
-1261 to -1277
-613
-430
-386 to -374
-355 to -333
-198
0
Signal Peptide
Prodomain
Catalytic Domain
Cys/His Rich Domain
E-Box
NF-Y
Sp1
SRE
HNF1α

Costet and colleagues demonstrated that PCSK9 is regulated by insulin status through SREBP-1c in rodent primary hepatocytes [79]. In the presence of insulin, *PCSK9* mRNA levels were shown to increase by 4-fold. SREBP-1c mediates this insulin response, through both SRE and a functional response element, the "E-box", found in the proximal promoter of *PCSK9* (Figure 4) [79]. In parallel studies conducted in rats, Persson and colleagues demonstrated that glucagon had an opposite effect, repressing mRNA *PCSK9* expression by 70% [87].

Studies conducted by Langhi and colleagues with the bile acid chenodeoxycholic acid (CDCA), and a synthetic agonist of Farnesoid X Receptor (FXR), demonstrated that *PCSK9* transcription could be repressed through activation of the FXR [88]. The authors coadministrated CDCA with statins and prevented statin induced upregulation of PCSK9 specifically.

Recently, Li and colleagues identified that *PCSK9* is responsive to HNF1α. In their studies, they identified a cis-regulatory site upstream of the SRE, which upon deletion repressed *PCSK9* expression (Figure 4) [81]. In this region an HNF1α binding site was identified at -386 to -374bp of the proximal promoter. *PCSK9* is the first gene identified in cholesterol metabolism which utilizes HNF1α cooperatively with SRE [81]. This group concluded that HNF1α promoted *PCSK9* transcription, and that HNF1α was important in the sterol-dependent regulation of PCSK9.

1.2.3 Proprotein Convertase Subtilisin/Kexin 9 Biosynthesis

While many studies have focused on PCSK9 transcriptional regulation, the study of its post-translational regulation is equally important since PCSK9 post-translationally regulates LDLR degradation [47, 49, 79-81, 88]. Any factor which may increase or decrease the half-life of PCSK9 can act independently of transcriptional regulation to further modulate PCSK9 levels or its availability for LDLR binding and subsequently PCSK9 mediated LDLR degradation.

Figure 5 illustrates PCSK9 domain structure, and its maturation from a ~74kDa proprotein to a ~60kDa processed form, through the secretory pathway. With its discovery in 2003, biosynthesis studies showed that PCSK9 was glycosylated at Asn533 (Figure 5) [12]. Further analyses showed sulfation of PCSK9 and its propeptide at Tyr38 [32]. Unique to PCSK9, the propeptide is not cleaved at a secondary site to release it from occupying the binding pocket of the catalytic domain, and so PCSK9 is secreted into circulation tightly associated with its propeptide as a catalytically inactive convertase [12, 32]. Neither the presence/absence of glycosylation, nor sulfation of PCSK9 has been demonstrated to affect its function; that is PCSK9 mediated: LDLR degradation [89]. We were the first to demonstrate that PCSK9 is secreted as a phosphoprotein [90]. We showed two sites of PCSK9 phosphorylation; Ser47 in the propeptide, and Ser688 in its C-terminal Cys/His-rich domain (CHRD) (Figure 5) [90]. Identifying the sites of phosphorylation, minimal consensus sequence recognized, and identifying the role(s) of phosphorylation in PCSK9 function is the focus of this thesis and will be discussed further in subsequent sections.

Figure 5. Schematic of PCSK9 Biosynthetic Pathway. Schematic showing maturation of proPCSK9 through secretory pathway. PCSK9 autocatalytically cleaves itself at the junction between its prodomain and catalytic domain (VFAQ↓SIP) in the ER. As PCSK9 passes through the ER it is glycosylated at Asn533. In the Golgi this glycosylation is further maturated. While in the *trans*-Golgi, PCSK9 is sulfated at Tyr38 in its propeptide and at an unknown site in PCSK9. Phosphorylation occurs at two sites; Ser47 in the propeptide and Ser688 in the C-terminus. PCSK9 is secreted as a heterodimer, complexed with its prodomain. A truncated inactive form of PCSK9 has been reported which is cleaved by PCSK3/Furin at the consensus motif RFHR218 resulting in an ~50kDa fragment.

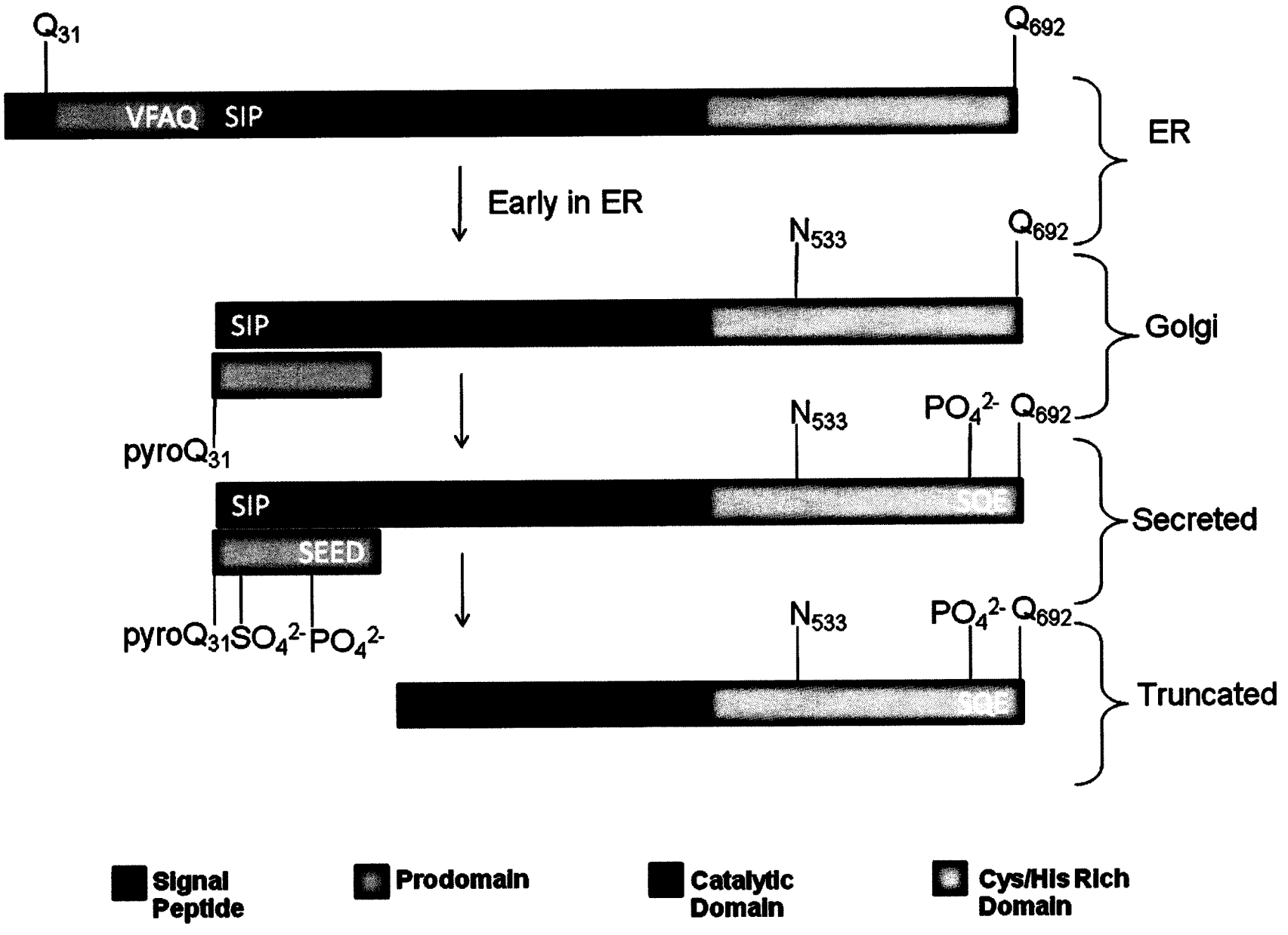
Q_{31}
Q_{692}
VFAQ
SIP
ER
Early in ER
N_{533}
Q_{692}
SIP
Golgi
N_{533}
PO_4^{2-} Q_{692}
pyroQ_{31}
SIP
SEED
Secreted
pyroQ_{31} SO_4^{2-} PO_4^{2-}
N_{533}
PO_4^{2-} Q_{692}
Truncated
Signal Peptide
Prodomain
Catalytic Domain
Cys/His Rich Domain

1.2.4 Proprotein Convertase Subtilisin/Kexin 9 Mechanism(s) of Action

Although the exact mechanism(s) are not known, PCSK9 modulates plasma LDLC levels by affecting post-translational levels of LDLR [32, 49]. As mentioned earlier, missense 'gain of function' SNPs of *PCSK9* predisposed human carriers to hypercholesterolemia by enhancing LDLR degradation [32, 66, 91, 92] while missense and nonsense 'loss of function' SNPs associated with hypocholesterolemia by reducing LDLR degradation [52, 91]. The initial association of 'gain of function' mutations in PCSK9 with hypercholesterolemia was the first indication of the importance of PCSK9 in cholesterol homeostasis.

Studies in mouse models provided insight into the mechanism and site(s) of action of PCSK9 in cholesterol homeostasis [32, 47, 49, 50, 79]. Knockout mouse (KO) studies demonstrated that PCSK9 indirectly affected plasma LDLC levels by promoting the post-transcriptional degradation of LDLR [47]. While LDLR mRNA levels were unaltered, LDLR protein levels in PCSK9 KO mice were 2.8-fold higher than wild-type, and as a result plasma LDLC levels were reduced by ~40% in these mice [47]. This was due to the efficient recycling of LDLR protein in the absence of PCSK9. In contrast, adenovirally-mediated overexpressing of PCSK9 exhibited the opposite phenotype - hypercholesterolemia- with decreased LDLR protein levels (but not LDLR mRNA) resulting in a 2-fold increase in plasma LDLC levels [32, 49, 50].

While autocatalytic activity is required for PCSK9 to exit the ER [12, 32, 93], PCSK9 catalytic activity is not required for PCSK9: mediated LDLR degradation [93]. As mentioned

earlier, PCSK9 is secreted with its propeptide tightly associated with its catalytic domain, and is thus enzymatically inactive [12]. In fact, several studies have demonstrated that engineered, catalytically inactive PCSK9 mutants either injected *in vivo*, or that were overexpressed *ex vivo* in HEK 293 cells and added to media containing HepG2 cells are capable of promoting LDLR degradation similar to wild type hPCSK9(WT) [93, 94]. At the cell surface, the conformation of the PCSK9: propeptide complex favours interaction of a region of the catalytic domain of PCSK9 (distinct from the catalytic pocket) with the epidermal growth factor-A (EGF-A) domain of LDLR, a site different than the region of LDLR that binds to LDLC, and this complex is endocytosed (Figure 2) [95]. Crystal structure studies of PCSK9 complexed to the EGF-A domain of LDLR demonstrated this *in vitro* [96, 97]. Residues R194 and F379 of PCSK9 are important for this binding to occur [96]. *Ex vivo* studies demonstrated that the PCSK9(D374Y) which causes ADH, binds to this site on LDLR 10-25X more strongly than PCSK9(WT) (Kd=170nm) at the cell surface, identifying its mode of action [98]. Mutation PCSK9(D374Y) promotes a favourable hydrogen bond between PCSK9 and His306 of LDLR, thus increasing the affinity of D374Y-PCSK9 for LDLR [96]. Furthermore, the binding affinity of PCSK9(WT) for LDLR was shown to increase in more acidic environments, such as the late endosomes (Kd= 1nm), in contrast to LDL-C, which when bound to LDLR dissociates at low pH [95, 98]. Thus the PCSK9: propeptide complex acts as a chaperone to redirect the LDLR from recycling compartments toward the late endosomal compartments where ultimately the entire complex is degraded in the lysosome [95, 99].

While the above studies focused on the interaction of LDLR with PCSK9 at the cell surface and in the endosomes, one study has suggested that PCSK9 may affect LDLR levels

intracellularly [49]. This was based on their finding that in the absence of the ARH adapter protein (found at the cytoplasmic surface of the plasma membrane and required for internalization of LDLR), mice overexpressing PCSK9 still caused LDLR degradation [49]. Recent studies by Poirier and colleagues provide support for an intracellular pathway [100]. When ARH adaptor protein was knocked down in HepG2 cells using small interfering RNA (si-RNA), rather than an increase in LDLR levels, no change in LDLR levels was observed. This was in agreement with the previous results from ARH KO mice, suggesting PCSK9 may promote LDLR degradation through an ARH-independent intracellular pathway [49].

Other studies suggest that the extracellular pathway is more prominent in PCSK9 mediated LDLR degradation. Lagace and colleagues performed experiments, where they parabiosed a transgenic mouse overexpressing human PCSK9 to a wild-type (WT) mouse [92]. After parabiosis, very low levels of hepatic LDLR were detected in WT mice, demonstrating that PCSK9 secreted into circulation by the transgenic mouse was capable of promoting degradation of hepatic LDLR in the adjoining WT mouse. A peptide developed against the EGF-A domain of LDLR is capable of interfering with PCSK9: LDLR binding in both HepG2 and HEK293 cells [97, 101]. McNutt and colleagues demonstrated that addition of an EGF-A peptide to the medium of HepG2 cells overexpressing PCSK9 was capable of interfering with secreted PCSK9 mediated LDLR degradation, leading to a recovery of LDLR levels similar to controls [97]. Pulse-chase analysis of ^{125}I-EGFAB(H306Y) peptide in the absence of PCSK9 revealed that negligible amounts of this peptide were cell associated, or recovered as mono-^{125}I from the media as a result of intracellular metabolism, indicative that this peptide was acting only at the cell surface [97].

Chan and colleagues developed a monoclonal PCSK9 antibody against an epitope near the region of interaction to LDLR [102]. When administered to the medium of HepG2 cells *in vitro*, or injected into mice or cynomolgus monkeys *in vivo*, this PCSK9 antibody was capable of blocking secreted PCSK9 from binding to LDLR, effectively attenuating PCSK9 mediated LDLR degradation [102]. Relative to untreated HepG2 cells overexpressing PCSK9, HepG2 cells treated with this PCSK9 antibody led to a 10.2-fold increase in LDLR protein levels [102]. In mice injected with the PCSK9 antibody, a 2.3-fold increase in hepatic LDLR protein levels was observed compared to controls, and in monkeys, the PCSK9 antibody led to significantly reduced serum total cholesterol levels [102]. These data demonstrate the importance of the extracellular pathway in PCSK9-mediated LDLR degradation.

1.2.5 Post-Translational Regulation of PCSK9

The availability of free circulating PCSK9 can modulate its interaction with and mediation of LDLR degradation. Understanding endogenous means of regulating levels of circulating PCSK9 are thus important, and provide avenues to pursue drug development of PCSK9 inhibitors. Such endogenous modes of regulating availability of circulating protein can include susceptibility to protease digestion which can affect the half-life of the protein, and interacting partners which can sequester the protein from LDLR.

1.2.5.1 Post-translational Cleavage By PCSK3/Furin

The PCSK9 'gain of function' mutant hPCSK9(D374Y) has enhanced binding affinity for the EGFA domain of LDLR, however this mode of action does not explain other 'gain of function' variants, nor 'loss of function' variants for that matter. It was possible that *PCSK9* SNPs encoding other 'gain of function' or 'loss of function' PCSK9 variants may enhance or abrogate processing events which modulate PCSK9 expression or half-life. In HEK 293 and CHO K1 cell lines overexpressing hPCSK9, Benjannet and colleagues observed a secreted, truncated form of PCSK9 (Figure 5) [89]. Levels of this truncated PCSK9 were significantly reduced in these cell lines overexpressing the 'gain of function' mutants hPCSK9(R218S) and hPCSK9(F216L), compared to hPCSK9(WT) [89]. Analysis of the sequence revealed a conserved motif, RFHR218, recognized by PCSK3/Furin. Immunoblotting showed this truncated form of PCSK9 was ineffective in promoting LDLR degradation compared to PCSK9(WT), while the hPCSK9(R218S) (which prevents this cleavage), and hPCSK9(F216L) (which greatly reduced this cleavage), promoted LDLR degradation greater than WT-PCSK9. Their results suggested that PCSK9 is post-translationally cleaved by Furin into an inactive form which can not mediate LDLR degradation. Therefore the loss of, or reduction in this cleavage event, as with PCSK9 Furin-cleavage site mutants hPCSK9(R218S) and hPCSK9(F216L), promoted a 'gain of function' phenotype, while enhanced Furin-cleavage would promote the opposite 'loss of function' phenotype.

1.2.5.2 Annexin A2

The interaction of the PCSK9: propeptide complex with LDLR to promote its degradation is well documented [32, 49, 93, 95]. Mayer and colleagues reported that PCSK9 interacts with another protein found at the cell surface, annexin A2, a member of the Ca^{2+}-dependent, membrane binding annexin family [103]. Annexin A2 is a ~36kDa membrane associated protein that affects functions including plasmin activation, angiogenesis and fibrinolysis [104-106].

Annexin A2 contains a 3kDa N-terminal "tail domain" which is distinct from other annexin family members, and a highly conserved 33kDa C-terminal core domain of four Ca^{2+} binding repeats necessary for membrane association [105]. While Annexin A2 does not have a signal peptide sequence, and has not been detected in the secretory pathway, it nonetheless is capable of constitutively translocating to the plasma membrane provided upon heterotetramerization with its S100 partner protein p11, and Tyr phosphorylation at Tyr23, but not Ser25 phosphorylation [107, 108]. The Ca^{2+} binding ability of endonexin repeat domain 2 in the C-terminus is required to anchor Annexin A2 to phospholipids in the plasma membrane [108]. Heterotetramerization of annexin A2 with another annexin A2/p11 heterodimer is facilitated by interactions with the N-terminus of Annexin A2 [109].

Mayer and colleagues demonstrated through far western analysis that the C-terminal domain of PCSK9 bound to the N-terminal domain of annexin A2, sequestering PCSK9 at the cell surface [103]. This interaction was specific for annexin A2, as PCSK9 did not bind the family member annexin A1 which shares ~53% sequence homology with annexin A2.

Annexin A2 transiently transfected into HepG2 cells, resulted in increased LDLR levels, while in untransfected HepG2 cells where annexin A2 is absent, LDLR levels were correspondingly reduced, demonstrating annexin A2 is an endogenous inhibitor of PCSK9 action [103].

It has been noted previously that cell lines and tissues respond differently to PCSK9 with respect to PCSK9 mediated LDLR degradation [49, 94, 110]. Mayer and colleagues correlated this in cell culture to respective differences in levels of available annexin A2 [103]. This may explain why in the adrenal gland, which has comparable levels of LDLR as in liver but has much higher levels of annexin A2, no significant effect is observed with regards to PCSK9-mediated LDLR degradation [94].

1.3 Phosphorylation

1.3.1 Protein Phosphorylation and Function

The first phosphorylated protein, casein, was identified from milk extract in 1883 [111], but it was nearly one hundred years later that the first protein kinase was discovered, and subsequently the mechanism of transfer of a phosphoryl group from ATP to the phospho-receptive amino acid was determined [112, 113]. There are three phospho-receptive amino acids: serine, threonine, and tyrosine [112, 114, 115]. In a recent phospho-amino acid study, the approximate distribution of phosphoserine, phosphothreonine, and phosphotyrosine residues in the human proteome was 86.4, 11.8, and 1.8% respectively [116].

Reversible protein phosphorylation plays diverse functional roles within the cell. Through allosteric conformational changes mediated by the steric size and negative charge of the addition of a phosphoryl group, phosphorylation can activate/deactivate enzymes [117], participate in cellular signal transduction events [118], alter protein stability [119, 120], affect sub-cellular localization [121], and modulate protein-protein interactions [122].

Protein phosphorylation is modulated through the action of protein kinases (phosphorylate) and phosphatases (dephosphorylate). With the sequencing of the human genome and since the subsequent identification of the human kinome in 2002, the eukaryotic protein kinases have been classified according to several groups, AGC family, PKC family (Protein Kinase C family), CAMK (Ca++/Calmodulin regulated kinases), CK1 (Casein Kinase I family), MAPKs (mitogen activated protein kinases), GSK (glycogen synthase kinase), and tyrosine kinases [123]. Many of these kinases are cytosolic, but some are membrane associated and/or compartmentalized.

1.3.2 Phosphorylation of Secreted Proteins

Phosphorylation events can occur at several points along the secretory pathway from ER, to the Golgi, or in the extracellular environment after secretion. Several proteins processed through the secretory pathway are phosphorylated in the Golgi, including among others insulin-like growth factor binding proteins (IGFBPs), osteopontin, aquaporin, the PCSK2 chaperone protein 7B2, and PCSK3/Furin [122, 124-128]. For members of the IGFBP family such as IGFBP-1 or -3, phosphorylation promotes increased binding affinity for their target protein, insulin growth factor [128]. For PCSK3/Furin, which is phosphorylated at its C-

terminal tail, phosphorylation acts a translocation signal, altering its trafficking from cell surface to the TGN [126]. Phosphorylation of the PCSK2 chaperone protein 7B2, reduces its binding affinity for PCSK2, which promotes PCSK2 activation [122].

1.3.3 PCSK9 is a Phosphoprotein

Proprotein convertase subtilisin/kexin type 9 (PCSK9) degrades LDLR through a lysosomal dependent pathway [99]. The detailed mechanism and physiological conditions that might modulate the function of PCSK9 in this process are still being elucidated. As previously discussed, the transcriptional regulation of PCSK9 has been the focus of several studies; most have explored its co-directional regulation with the LDLR by SREBP-2, while others have demonstrated that PCSK9 can be regulated through alternate pathways including the SREBP-1c, FXR, and HNF1α pathways [79-81, 88]. To further understand its cell biology and mechanism of action we decided to analyze the post-translational regulation of PCSK9 based on our novel finding that PCSK9 is a phosphoprotein.

1.4 Hypothesis and Objectives

1.4.1 Hypothesis

We propose that PCSK9 circulates in several molecular forms (such as phosphorylated and unphosphorylated) and that these molecular forms can affect its subsequent effect on LDLR, shifting the equilibrium between LDLR recycling and LDLR degradation.

1.4.2 Objectives

Herein I used a combination of site directed mutagenesis (SDM), mass spectrometry, immunoblotting and metabolic labeling to:

1) Identify the sites of PCSK9 phosphorylation, and determine the consensus motif of the kinase responsible.

2) Determine the effect of phosphorylation on PCSK9 processing, secretion and stability.

3) Use SDM to produce mutants which will be used in a functional assay of PCSK9 phosphorylation.

4) Study the effect of phosphorylation status on the Interaction between PCSK9 and the cell-surface protein Annexin A2.

2. Materials and Methods

2.1 Constructs and Antibodies

The cDNA of human PCSK9 was cloned into the pIRES2-enhanced green fluorescent protein with or without a C-terminal V5 tag and provided as a kind gift from Dr. N.G. Seidah. Mutations were introduced by site-directed mutagenesis (SDM, Stratagene Product Number: 200518-5) following Stratagene protocol (Table 2).

Table 2. PCSK9 Mutants Engineered By Site-Directed Mutagenesis

PCSK9 Residue	Mutant Residue	Primer Direction	Primer Sequence
S47	A	Sense	TGGTGCTAGCCTTGCGTGCCGAGGAGG
		Antisense	CCTCCTCGGCACGCAAGGCTAGCACCA
	D	Sense	AGCTGGTGCTAGCCTTGCGTGACGAGGAGGACG
		Antisense	CGTCCTCCTCGTCACGCAAGGCTAGCACCAGCT
	E	Sense	GTGCTAGCCTTGCGTGAGGAGGAGGACGGCCTG
		Antisense	CAGGCCGTCCTCCTCCTCACGCAAGGCTAGCAC
E48	A	Sense	CCTTGCGTTCCGCGGAGGACGGCCT
		Antisense	AGGCCGTCCTCCGCGGAACGCAAGG
	D	Sense	CCTTGCGTTCCGACGAGGACGGCCT
		Antisense	AGGCCGTCCTCGTCGGAACGCAAGG
E49	A	Sense	GCGTTCCGAGGCGGACGGCCTGG
		Antisense	CCAGGCCGTCCGCCTCGGAACGC
	D	Sense	GCGTTCCGAGGATGACGGCCTGGCC
		Antisense	GGCCAGGCCGTCATCCTCGGAACGC
D50	A	Sense	TTCCGAGGAGGCCGGCCTGGCCG
		Antisense	CGGCCAGGCCGGCCTCCTCGGAA
	E	Sense	GCGTTCCGAGGAGGAGGGCCTGGC
		Antisense	GCCAGGCCCTCCTCCTCGGAACGC
S688	A	Sense	TGGCGCAGGCCGCCCAGGAGCTC
		Antisense	GAGCTCCTGGGCGGCCTGCGCCA
	D	Sense	TGGCGCAGGCCGACCAGGAGCTC
		Antisense	GAGCTCCTGGTCGGCCTGCGCCA
	E	Sense	CACCTGGCGCAGGCCGAGCAGGAGCTCCAGTGA
		Antisense	TCACTGGAGCTCCTGCTCGGCCTGCGCCAGGTG
E690	A	Sense	CAGGCCTCCCAGGCGCTCCAGTGACAG
		Antisense	CTGTCACTGGAGCGCCTGGGAGGCCTG
	D	Sense	CAGGCCTCCCAGGATCTCCAGTGACAGAA
		Antisense	TTCTGTCACTGGAGATCCTGGGAGGCCTG
S47/S688	A/A[¥]	Sense	TGGCGCAGGCCGCCCAGGAGCTC
		Antisense	GAGCTCCTGGGCGGCCTGCGCCA
	D/D[§]	Sense	TGGCGCAGGCCGACCAGGAGCTC
S47/S688		Antisense	GAGCTCCTGGTCGGCCTGCGCCA
	E/E[£]	Sense	CACCTGGCGCAGGCCGAGCAGGAGCTCCAGTGA
		Antisense	TCACTGGAGCTCCTGCTCGGCCTGCGCCAGGTG
D374	Y	Sense	CATTGGTGCCTCCAGCTATTGCAGCACCTGCTTTG
		Antisense	CAAAGCAGGTGCTGCAATAGCTGGAGGCACCAAT
R46	L*	--	--
A53	V*	--	--
Y38	F*	--	--

* Gifts kindly provided by Dr. N.G. Seidah

[¥] PCSK9(S47A) used as template instead of PCSK9(WT)

[§] PCSK9(S47D) used as template instead of PCSK9(WT)

[£] PCSK9(S47E) used as template instead of PCSK9(WT)

Mutated PCSK9 constructs were verified by DNA Sequencing service provided by BioBasic Inc (Markham, Ontario). Stocks of PCSK9 mutant DNA were diluted to 100ng/ul, and aliquotted into a 96-well plate. Primers used to sequence PCSK9 constructs were diluted to 10μM and provided separately to BioBasic for sequencing analysis (Table 3). Both ChromasLite and NCBI sequence alignment BLAST software were used to analyze sequencing data provided by BioBasic to verify the site directed mutagenesis as well as the integrity of the PCSK9 construct.

Table 3. Primers Used for Sequencing of PCSK9 Plasmid Constructs

Primer ID	Primer Sequence
B-PCSK9-R	TCCCGGTGGTCACTCTGTAT
C-PCSK9-F	ATACAGAGTGACCACCGGGA
D-PCSK9-R	TGGATCAGTCTCTGCCTCAA
E-PCSK9-F	TTGAGGCAGAGACTGATCCA
F-PCSK9-R	CTGGCAATGGCGTAGACAC
G-PCSK9-F	GTGTCTACGCCATTGCCAG

Anti-hPCSK9 Ab, used for the immunoprecipitation of endogenous or untagged recombinant PCSK9 was previously raised in rabbits by cDNA vaccination with the mammalian expression vector pcDNA3 into which the cDNA for human PCSK9 had been inserted [129]. The mouse anti-V5 Ab used for immunoprecipitation of V5-tagged recombinant PCSK9 was from Invitrogen (Burlington, Canada) and the goat anti-(C-terminal PCSK9) Ab used for immunoblotting from Imgenex (San Diego, CA, USA) (Table 4). Secondary anti-mouse and anti- (rabbit HRP) Ab were from Amersham (Piscataway, NJ, USA) and the secondary anti-(goat HRP) Ab was from Santa Cruz Biotechnology (Santa Cruz, CA, USA) (Table 4).

Table 4. List of Antibodies Used for Immunoprecipitation, and/or Immunoblotting

Primary Antibodies	Manufacturer	Product Number
anti-hPCSK9 Ab (For WB)	Gift Kindly from Dr. N.G. Seidah	--
anti-hPCSK9 Ab (For IP)	In house Ab [129]	--
goat anti-(C-terminal) Ab	Imgenex	IMG-3786
mouse anti-V5 Ab	Invitrogen	46-0705
rabbit anti-LDLR Ab	Fitzgerald	20R-LR002
mouse anti-Transferrin Receptor	Invitrogen	13-6800

Secondary Antibodies	Manufacturer	Product Number
anti-mouseHRP Ab	Amersham	NA931V
anti-rabbitHRP Ab	Amersham	NA9340V
anti-goatHRP Ab	Santa Cruz Biotechnology	sc-2020

2.2 Cell culture, Transfection and Sample Collection

HepG2, HuH7, HEK293 and CHOK1 cells were grown at 37 ^{0}C in Dulbecco's modified Eagle's medium (DMEM) + 10% Fetal Bovine Serum(FBS) + gentamycin (28 μg/mL). Cells (3 x 10^{5}) were transfected with a plasmid expression vector for human PCSK9 (hPCSK9; 4 μg) as described using Lipofectamine 2000 (Invitrogen) in a 1:1 ratio with Lipofectamine. Spent media from untransfected and transfected cells were collected in the presence of a general protease inhibitor cocktail (Roche, Laval, Canada) and 200 μM sodium orthovanadate (a phosphatase inhibitor; Sigma-Aldrich, Oakville, Canada) and centrifuged at 13 000 g for 3 min to remove suspended cells and debris. Cells were lysed in 1x RIPA buffer (50 mM Tris pH 7.6, 150 mM NaCl, 1% v / v NP-40, 0.5% w/ v deoxycholate, 0.1% w/ v SDS) in the presence of inhibitors, as above. Lysates were rotated at 4 ^{0}C for 10 min, centrifuged at 3 000 g for 10 min and supernatants collected. Protein concentrations in total

cell lysates were determined by the Bradford dye-binding method using Bio-Rad's Protein Assay Kit (Bio-Rad, Mississauga, Canada).

2.3 Immunoprecipitation, Immunoblotting and Radiolabeling

Immunoprecipitations were carried out in 1x Tris-buffered saline(50mM Tris, 100mM NaCl pH-7.6) + 0.1% Tween-20 with anti-hPCSK9 Ab (dilution 1:500), preimmune sera (dilution 1:500) or anti-V5 IgG (1:500) and 30 μL of protein A agarose (Sigma-Aldrich) overnight at 4 ^{0}C. Immunoprecipitates were washed 4x with 1 mL 1x Tris-buffered saline + 0.1% Tween-20 and fractionated through a 10% polyacrylamide gel for 1.5 hrs at 150V (constant voltage). Proteins were electroblotted onto nitrocellulose at 30V overnight at 4 ^{0}C, and immunoblotted following a standard protocol. Immunoblots were incubated in blocking buffer (5% milk in 1x Tris Buffered Saline + 0.1% Tween-20) for 45 minutes followed by incubation in either primary anti-(C-terminal PCSK9) or primary anti-V5 Ab (used at 1:2000 dilution in blocking buffer) for 1hr. After washing 3x in 1x Tris buffered saline+ 0.1% Tween-20, immunoblots were incubated in secondary antibodies at 1:5000 dilutions for 1hr at room temperature. Immunoblots were revealed by chemiluminescence using Western Lightening Plus (Perkin-Elmer, Woodbridge, Canada) on Kodak X-OMAT film (VWR International, Montreal, Canada). The signal was quantified by densitometry using Syngene's Chemigenius 2XE imager and Genetool software (VWR International).

Untransfected and transfected HepG2 and HuH7 cells were grown to confluence as above. Prior to radiolabeling cells were incubated for 4 h in serum-free DMEM without sodium phosphate (Invitrogen) or 45 min Cys /Met-free Dulbecco's modified Eagle's medium

(Invitrogen) and then incubated for various times in the same media in the presence of either 250 μCi ^{32}P-orthophosphate or 250 μCi ^{35}S- Cys /Met. Media and total cell lysates were harvested and immunoprecipitated as described above. Samples were fractionated through a 12% SDS / PAGE. Following electrophoresis, gels were dried under vacuum at 50^{0}C, and visualized by phosphorimaging using a Typhoon Imager. Signals were quantified using Imagequant 5.2 software using the integer integration method when comparing samples within a lane and, for samples between lanes by volume quantitation, as recommended.

2.4 Far Western Analysis

Untransfected and transfected HepG2, HEK293 and HuH7 cells were grown to confluence as above. Spent media from cell cultures of HuH7 cells untransfected or transfected with an hPCSK9 expression vector were collected and immunoprecipitated as above for Far Western Analysis. Total cell lysates from untransfected HuH7 cells were fractionated through a 4-12% Tris-Acetate gel (Invitrogen) and electroblotted onto nitrocellulose. Immunoblot was incubated in blocking buffer followed by incubation with 0.5 μg/ml of either spent media containing hPCSK9(WT) or hPCSK9(S47A/S688A) for 3 hrs at room temperature. Immunoblots were washed 3 times in 1 times Tris buffered saline + 0.1% Tween-20 and incubated for 1 hr in primary antibody anti-PCSK9 Ab at 1:1000 dilution. After washing 3 times in 1x Tris buffered saline + 0.1% Tween-20, immunoblots were incubated in secondary anti-rabbit HRP conjugated Ab at 1:5000 dilution for 1hr at room temperature. Immunoblots were developed by chemiluminescence and signal was quantified by densitometry as described above.

2.5 Mass Spectrometry Analyses

Spent media from cell cultures of HepG2, HuH7, HEK293 and CHOK1 cells untransfected or transfected with an hPCSK9 expression vector were collected and immunoprecipitated as above for Time Of Flight-MS (TOF-MS) analysis of immunocaptured PCSK9 as previously described, except that following immunoprecipitation, the antibody / antigen complex was eluted from the protein A beads by incubation in 2x 150 µL of 0.1 M glycine (pH 2.8) for 10 min at room temperature. Supernatants were collected, combined and neutralized with 30 µL 1M Tris / HCl (pH 9.0), concentrated 20x with an Amicon Ultra YM10 Centricon (Millipore Corp., Temecula, CA, USA) and retentates equilibrated in 0.1% trifluoroacetic acid. Ten microliters of the sample was applied to a Gold ProteinChip Array (Ciphergen Biosystems Inc., Fremont, CA, USA) and air-dried. One microliter of saturated 3, 5-dimethoxy-4-hydroxycinnamic acid in 50% (v / v) acetonitrile + 0.5% (v / v) trifluoroacetic acid was added and samples analysed by TOF-MS in a Ciphergen Protein Biology System II. Analyses represent an average of 100 shots and masses were externally calibrated with All-in-1 Protein Standards (Ciphergen Biosystems Inc.). All data were normalized for total ion current and peak areas calculated using the indirect method (with a bracket height of 0.4 and width expansion factor of 2) contained within Ciphergen's Proteinchip 3.1 software.

2.6 Dephosphorylation

Enzymatic dephosphorylation was carried out by incubating immunoprecipitates in the presence of 10 units (except where indicated) of shrimp alkaline phosphatase (SAP)

(Fermentas, Burlington, Canada) in the provided 10x reaction buffer system (diluted to 1x with dH_20) for 30 min at 37 ^{0}C with agitation.

2.7 Trypsin Digestion

Trypsin digestion was carried out by incubating immunoprecipitates in the presence of 6 ng/μL trypsin (Roche) in 25 mM NH_4HCO_3 and 1% (v / v) acetonitrile overnight at 37 ^{0}C with agitation.

2.8 Statistical Analyses

All results are expressed as mean ± standard error (SE), except where indicated. Data were analyzed using Graphpad Prism 5.0 statistical software with significance defined as $P < 0.05$.

3. Results

3.1 Phosphorylation of PCSK9

3.1.1 Secreted PCSK9 Propeptide is Phosphorylated

Initial characterization of PCSK9 by Seidah and colleagues in 2004 identified that it was N-glycosylated at N533 in its C-terminal domain, and sulfated at Y38 in its prodomain (Figure 5) [32]. Mass spectrometry (MS) performed by our group on the propeptide: secreted PCSK9 complex from HepG2 cells demonstrated that the propeptide was secreted predominantly in two molecular forms [32]. One molecular form of PCSK9 propeptide represented sulfation at Y38 [89]. The second major molecular form from the MS analysis of PCSK9 propeptide was modified with another functional group other than sulfation but that could contribute to an 80Da addition [90]. Addition of a phosphoryl group could account for this heterogeneity [90].

To determine whether the PCSK9 propeptide was phosphorylated, we immunoprecipitated spent media from HepG2 cells with anti-hPCSK9 antibody (Ab) as described in materials and methods. Immunoprecipitates were divided in half and one-half treated with shrimp alkaline phosphatase (SAP) and then analysed by Time-of-Flight Mass Spectrometry (TOF MS) as described in materials and methods. Two peaks were visible in the mass spectral plot of PCSK9 propeptide in the absence of SAP treatment, at 13 834.6 Da and 13 915.5 Da, corresponding to sulfated (SO_4^{2-}) PCSK9 propeptide and SO_4^{2-}PCSK9 propeptide with an

Figure 6. MS analysis of Molecular Mass Heterogeneity of Secreted PCSK9 Propeptide. (A–D) TOF-MS analyses of the molecular forms of endogenously expressed PCSK9-propeptide immunoprecipitated from the media of HepG2 cells with either immune (antihPCSK9 IgG; A, C) or preimmune sera (B, D), and following dephosphorylation (C, D). (E–H) TOF-MS analyses of the molecular forms of the propeptide of V5-tagged PCSK9 immunoprecipitates from the media of transfected and overexpressing HepG2 (E), HuH7 (F), HEK293 (G) and CHOK1 (H) cells. The ratio of the sulfated (SO_4^{2-}) to sulfated and phosphorylated (PO_4^{2-}), calculated as the area under the peak, as described in materials and methods, is shown ± SE. Analyses were conducted on at least three independent experiments. ns, nonspecific peak.

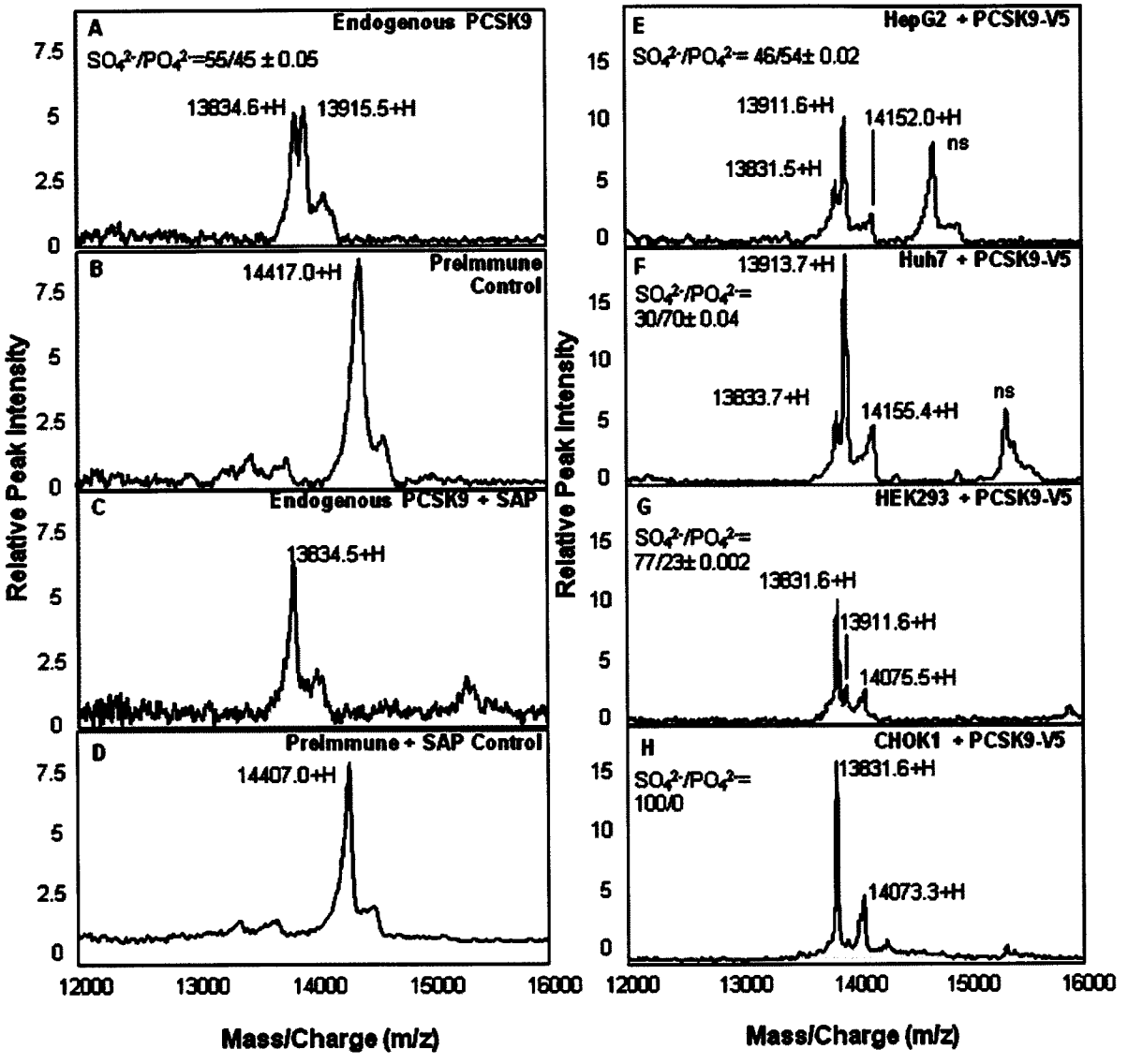
A
Endogenous PCSK9
SO_4^{2-}/PO_4^{2-}=55/45 ± 0.05
13834.6+H
13915.5+H
B
Preimmune Control
14417.0+H
C
Endogenous PCSK9 + SAP
13834.5+H
D
Preimmune + SAP Control
14407.0+H
E
HepG2 + PCSK9-V5
SO_4^{2-}/PO_4^{2-}= 46/54± 0.02
13911.6+H
14152.0+H
ns
13831.5+H
F
Huh7 + PCSK9-V5
13913.7+H
SO_4^{2-}/PO_4^{2-}= 30/70± 0.04
13833.7+H
14155.4+H
ns
G
HEK293 + PCSK9-V5
SO_4^{2-}/PO_4^{2-}= 77/23± 0.002
13831.6+H
13911.6+H
14075.5+H
H
CHOK1 + PCSK9-V5
SO_4^{2-}/PO_4^{2-}= 100/0
13831.6+H
14073.3+H
Relative Peak Intensity
Mass/Charge (m/z)

~80 Da addition, respectively (Figure 6A, calculated mass of SO_4^{2-}PCSK9: 13 835.5 Da with modification at pyroGlu31). A non-specific peak at 14 417 Da was seen by TOF MS analysis of immunoprecipitation of spent media with preimmune serum, as a control (Figure 6B). Examination of the immunoprecipitates by TOF MS of secreted PCSK9 propeptide treated with SAP revealed a single peak at size 13 834.5 Da (Figure 6C). This size corresponds to SO_4^{2-} PCSK9 propeptide (Figure 6A) and demonstrated that the second major molecular form of the PCSK9 propeptide at 13 915.5 Da (Figure 6A) represented sulfated and phosphorylated (SO_4^{2-}/ PO_4^{2-}) propeptide (calculated mass of SO_4^{2-}/ PO_4^{2-}PCSK9: 13 915.5 Da). Note that the molecular mass of the non-specific peak in Figure 6B did not change upon SAP treatment (Figure 6D). Analyses by TOF-MS of HepG2 total cell lysate did not identify phosphorylated PCSK9 propeptide (data not shown), suggesting that phosphorylation of PCSK9 propeptide occurred just prior to, or upon secretion.

3.1.2 Secreted PCSK9 Propeptide Phosphorylation is Cell-type Specific

Several cell lines are commonly used to study PCSK9 biosynthesis and function, including human embryonic kidney (HEK 293), Chinese hamster ovary (CHO K1), as well as the human hepatoma cell lines, HepG2 and HuH7 [49, 90, 92, 103]. With regard to PCSK9 mediated LDLR degradation, not all cell lines respond equally to PCSK9. Hepatic cell lines such as HepG2 cells respond more strongly to PCSK9 to promote LDLR degradation [49]. Having identified that the propeptide of PCSK9 was phosphorylated, we used the methodology mentioned above to determine whether phosphorylation status of PCSK9 propeptide differed between these cell lines. A previously constructed pIRES vector containing C-terminal V5-tagged wild-type PCSK9 (hPCSK9(WT)-V5, a kind gift from Dr.

N.G. Seidah, IRCM) was transiently transfected into HepG2, HuH7, HEK 293, and CHO K1 cells with Lipofectamine 2000 as per manufacturer's protocol and as described in materials and methods. We immunoprecipitated spent media from these cell lines with anti-V5 antibody (Ab) and immunoprecipitates were analysed by TOF MS as described in materials and methods.

As illustrated in Figure 6, both hepatoma cell lines produced two major peaks that corresponded to unphosphorylated but sulfated (SO_4^{2-}) PCSK9 propeptide and the sulfated and phosphorylated (SO_4^{2-}/ PO_4^{2-}) PCSK9 propeptide (13 831.5Da and 13 911.6Da respectively for HepG2; 13 833.7 Da and 13913.7 Da respectively for HuH7) (Figure 6E, F). Propeptide phosphorylation was confirmed in these cell lines by SAP treatment of immunoprecipitates (data not shown). Ciphergen PROTEINCHIP 3.1 software was used to analyze the area under the peak to compare the ratio of SO_4^{2-} to SO_4^{2-}/ PO_4^{2-} PCSK9 propeptide as described in materials and methods. Although SO_4^{2-} and PO_4^{2-} peptides can differ in their detection efficiency by TOF MS due to difference in charge, this difference is lost when comparing sizes greater than 8800 Da, validating this method of analysis [130]. Note that hPCSK9(WT)-V5 secreted by HepG2 cells is phosphorylated at a ratio of 46/54 $\pm$ 0.02 (n>3) (Figure 6A), similar to that produced endogenously (Figure 6E). This indicated that overexpression of PCSK9 did not affect propeptide phosphorylation status. The ratio of unphosphorylated to phosphorylated hPCSK9(WT)-V5 propeptide in HuH7 cells was 30/70 $\pm$ 0.04 ($p= 0.003$, n>3), suggesting more PCSK9 propeptide is secreted in the phosphorylated form with this cell line (Figure 6F). The ratio of unphosphorylated to phosphorylated hPCSK9(WT)-V5 propeptide in HEK 293 cells, was 77/23 + 0.002 ($p<0.0001$, n>3), suggesting that in contrast to the hepatoma cell lines, hPCSK9(WT)-V5 propeptide in HEK

293 is expressed predominantly in its sulfated state (Figure 6G). A phosphorylated form for hPCSK9(WT)-V5 propeptide was not detected from CHO K1 cells (Figure 6H). These results demonstrate that the PCSK9 propeptide is phosphorylated to different degrees between different cell lines tested. This can be attributed to cell-specific kinases and/or phosphatases involved in modulating PCSK9 phosphorylation status as well as varying levels of expression of those same kinases/phosphatases between cell lines tested.

Interestingly, two additional minor peaks are observed in these spectra at ~14 150 Da (Figure 6 E, F) and 14 070 (Figure 6 G, H), that corresponds to an alternative signal peptidase cleavage site following Ala28 (calculated mass 14 159.8 Da for SO_4^{2-}/ PO_4^{2-} PCSK9 propeptide, 14 079.8 Da for SO_4^{2-} PCSK9 propeptide). Indeed a signal peptide prediction program, SignalP 3.0 Server, predicted the primary cleavage of PCSK9 signal sequence at ARA30↓QE, but also predicted a secondary cleavage at A28↓RAQE. This alternative cleavage site was confirmed by N-terminal sequencing of PCSK9 propeptide bands excised from a PVDF membrane after electrophoresis (data not shown; N-terminal sequencing service provided by Dr. Claude Lazure, IRCM).

3.2 Identifying Site of PCSK9 Propeptide Phosphorylation and Critical Residues

3.2.1 Identifying Site of PCSK9 Propeptide Phosphorylation.

Having identified that the propeptide of PCSK9 was phosphorylated, we wanted to determine at which residue this modification occurred. Spent media from HepG2 cells transiently

transfected with hPCSK9(WT)-V5 was immunoprecipitated with anti-V5 antibody (Ab) as described in materials and methods. Half of the immunoprecipitates were treated with SAP, both halves were digested with trypsin, and analyzed by TOF MS as described in materials and methods. We used Client Paws 5.0 software to determine the calculated mass of tryptically cleaved products of the PCSK9 propeptide. We identified by TOF MS a tryptic fragment corresponding to pyroQ31-R66 of the PCSK9 propeptide, that shifted in size by 80Da after SAP treatment (observed mass at 4172.9 Da vs. calculated mass at 4174.2 Da) (Figure 7A, B, C). Several phospho-receptive residues are found within this region including three threonines, a tyrosine and a serine. We began with the serine residue for several reasons: 1) Arg-46-Leu (R46L), a known human variant of PCSK9 associated with hypocholesterolemia but with an unknown mode of action is found proximal to Ser47, 2) several proteins found in the secretory pathway are known to be phosphorylated by kinases recognizing either an S-X-X-D/E (Protein Kinase CK2) or S-X-E/Sp (Golgi Casein Kinase) motif, a sequence motif found in the prodomain of PCSK9, S47EED, 3) Tyr-38 is occupied by sulfation and 4) there were several Thr residues to choose from versus the single Ser residue.

Site-directed mutagenesis (SDM) (using the protocol from Stratagene) was used to engineer the phospho-mutant hPCSK9(S47A)-V5, using hPCSK9(WT)-V5 and primers as described in materials and methods. This construct was transiently transfected into HuH7 cells and V5-tagged PCSK9 was immunoprecipitated from spent media using anti-V5 antibody and immunoprecipitates were analysed by TOF MS as described in materials and methods. In spent media from HuH7 cells overexpressing hPCSK9(WT)-V5, two peaks were observed in

Figure 7. MS analysis of PCSK9-propeptide tryptic digests and phosphorylation site PCSK9-propeptide variant. (A, B) TOF-MS analyses of the tryptic peptides from the immunoprecipitates of the propeptide of V5-tagged PCSK9 from the media of transfected and overexpressing HuH7 cells in the absence (A) and presence (B) of SAP. (C) Amino acid sequence of the propeptide of PCSK9. pyroQ31, SO_4^{2-}, Y38 and PO_4^{2-}, Ser47 are in bold. The phosphorylated tryptic peptide is highlighted by red boxes in (A) and (B) and the corresponding amino acid sequence highlighted by a red font in (C). (D) MS analyses of the molecular form of the propeptide variant (S47A) of V5-tagged PCSK9 immunoprecipitates from the media of transfected and overexpressing HuH7 cells. Analyses were conducted on at least three independent experiments. ns, nonspecific peak.

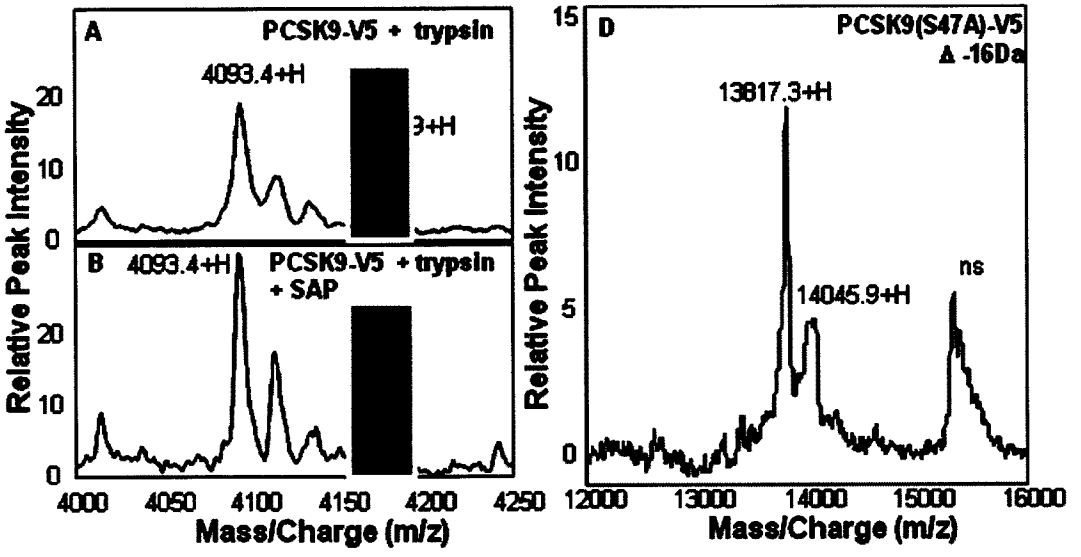

C

Q_{31}EDEDGDY[SO_4^{2-}]EELVLALRS[PO_4^{2-}]EEDGLAEAPEHGTTATFHR_{66}↓

CAKDPWRLPGTYVVVLKEETHLSQSERTARRLQAQAARRGYLTKILHV

FHGLLPGFLVKMSGDLLEALKLPHVDYIEEDSSVFAQ_{152}

a mass spectral plot for the propeptide of PCSK9, a peak of 13 833 Da representing SO_4^{2-} PCSK9 propeptide and a peak at 13 913 Da representing SO_4^{2-}/ PO_4^{2-} PCSK9 propeptide (Figure 6F). Analysis of hPCSK9(S47A)-V5 identified only a single peak of 13 817 Da (Figure 7C). The size difference for substitution of Ser for Ala is -16Da (calculated mass of SO_4^{2-} PCSK9(S47A): 13 818.5 Da), therefore this peak corresponded to the SO_4^{2-} PCSK9(S47A) propeptide, confirming S47 as the site of phosphorylation.

3.2.2 Determining Consensus Site for PCSK9 Prodomain phosphorylation

PCSK9 is found in the secretory pathway; kinases found in this pathway or at the cell surface include the casein kinase family of kinases. The well characterized protein kinase CKII (casein kinase II) is found at the cell surface and recognizes a consensus motif of S-X-X-D/E [131, 132]. The less known Golgi-casein kinase (GCK) is found within the Golgi apparatus and recognizes a consensus motif of S-X-E(Sp)/ or S-X-Q-XX-(E/D) [133, 134]. Having identified Ser47 as the phospho-receptive residue in the PCSK9 propeptide, the next step, given that the region surrounding the phosphoserine, S47EED, potentially matched consensus motifs for either GCK or CKII, was to determine whether the residues downstream of Ser47 affected its PO_4^{2-} and identify a consensus motif.

We assessed this by using SDM to substitute residues downstream of the phosphoserine for alanine to identify which residues were critical to phosphorylation. The EED residues downstream of Ser47 (hPCSK9(WT)-V5 as template) were individually substituted to either Ala or Asp, except for Asp50 which was substituted for Glu instead, to distinguish between consensus motif for CKII (S-X-X-D/E)and GCK (S-X-E) as described in materials and

methods (Table 2). These constructs were transiently transfected into HuH7 cells, and spent media collected after 72hrs as described in materials and methods. Analysis of immunoprecipitates from spent media by TOF MS revealed that neither substitution at E48 (to Ala or Asp) nor D50 (to Ala or Glu) affected phosphorylation status of PCSK9 prodomain as both SO_4^{2-} and SO_4^{2-}/ PO_4^{2-} peaks were still present (Figure 8A, B, C, F, G). A single peak however was observed in the mass spectral plot for E49 substituted with either Ala or Asp (Figure 8D, E). This peak corresponded to the calculated size of SO_4^{2-} hPCSK9(E49A)-V5 propeptide (calculated mass: 13 775.1 Da) and hPCSK9(E49D)-V5 propeptide (calculated mass: 13 822.3 Da), respectively. This demonstrated that the P+2 residue is selectively critical for PCSK9 propeptide phosphorylation, indicating a GCK-like kinase is responsible for phosphorylating PCSK9.

3.2.3 PCSK9 Propeptide Phosphorylation Status Is Decreased by Naturally Occurring Variations of PCSK9 Found in Proximity to Propeptide Phosphoserine

Our group showed that PCSK9 propeptide is secreted as a phosphoprotein into human plasma [90]. Two naturally occurring PCSK9 variants in the human population are found in the prodomain of PCSK9 at R46L, a 'loss of function' variant associated with hypocholesterolemia in Caucasians, and A53V, which is in complete linkage with Leu10 insertion in the signal peptide that is also associated with lower cholesterol levels in Caucasians [52, 129]. The mode of action of either hPCSK9(R46L) or hPCSK9(A53V) variants are unknown. Given that the R46L variant is located proximal to Ser47, and that A53V is located just downstream of the phosphoserine, we wanted to determine whether the phosphorylation status of hPCSK9(R46L)-V5 or hPCSK9(A53V)-V5 was affected.

Figure 8. MS analysis of the consensus site of PCSK9-propeptide phosphorylation from the media of transfected HuH7 cells overexpressing V5-tagged PCSK9 variants. (A–G) TOF-MS analyses of the propeptide of V5-tagged PCSK9 variants as labeled from the media of transfected and overexpressing HuH7 cells. For each variant the observed versus calculated (in brackets) molecular mass is shown below each panel for the sulfated (SO_4^{2-}) and sulfated and phosphorylated (PO_4^{2-}) propeptide, as well as the major molecular form observed. Analyses were conducted on at least three independent experiments. ACS, alternate signal peptidase cleavage site.

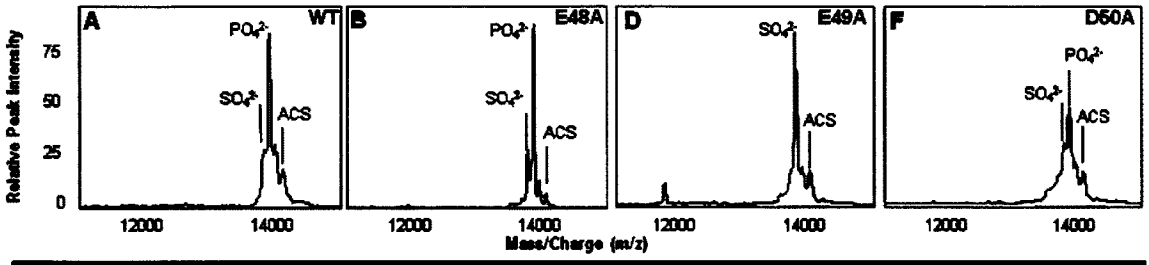

SO_4^{2-}	13827.9Da (13835.5Da)	13782.9Da (13777.5Da)	13775.1Da (13777.5Da)	13798.4Da (13791.5Da)
PO_4^{2-}	13906.4Da (13915.5Da)	13863.9Da (13857.5Da)	No PO_4^{2-} (13857.5Da)	13875.0Da (13871.5Da)
Form	phosphorylated	phosphorylated	sulfated	phosphorylated

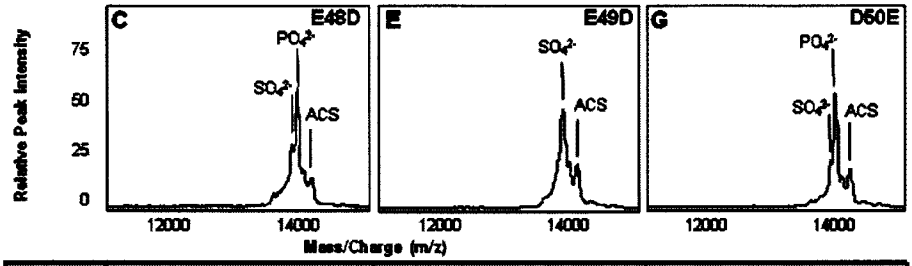

SO_4^{2-}	13822.2Da (13821.5Da)	13822.3Da (13821.5Da)	13853.3Da (13849.5Da)
PO_4^{2-}	13898.8Da (13901.5Da)	No PO_4^{2-} (13901Da)	13919.0Da (13929.5Da)
Form	phosphorylated	sulfated	phosphorylated

HuH7 cells were transiently transfected with hPCSK9(R46L)-V5, hPCSK9(A53V)-V5 or hPCSK9(WT)-V5 constructs and immunoprecipitates from spent media were analyzed by TOF MS as described in materials and methods. Ciphergen PROTEINCHIP 3.1 software was

used to analyze the area under the peak to compare the ratio of unphosphorylated to phosphorylated PCSK9 propeptide for both hPCSK9(R46L)-V5 and hPCSK9(A53V)-V5 in comparison to hPCSK9(WT)-V5 as described in materials and methods (Figure 9). Compared to hPCSK9(WT)-V5, the propeptide of hPCSK9(R46L)-V5 is 34% less phosphorylated ($p=0.0001$), while hPCSK9(A53V)-V5 is 17% less phosphorylated ($p=0.04$). hPCSK9(R46L)-V5 propeptide was also significantly less phosphorylated compared to hPCSK9(A53V)-V5. Thus, substitution of the P1 residue Arg for Leu is capable of significantly reducing the phosphorylation status of the PCSK9 propeptide, suggesting residues proximal to the consensus motif of PCSK9 propeptide can affect recognition by its cognate kinase. Also hPCSK9(A53V)-V5 demonstrates that residues downstream of the propeptide phosphoserine can affect this post-translational modification as well, since phosphorylation was significantly reduced in this mutant compared to hPCSK9(WT)-V5 ($p=0.04$).

Our group first demonstrated that the PCSK9 propeptide was sulfated at Tyr38 [89]. An engineered mutant hPCSK9(Y38F)-V5 produced an unsulfated PCSK9 propeptide. To determine whether sulfation at Tyr38 affected phosphorylation status of PCSK9, hPCSK9(Y38F)-V5 (a kind gift from Dr. N.G. Seidah) was studied. HuH7 cells were transiently transfected with hPCSK9(Y38F)-V5 or hPCSK9(WT)-V5 construct and immunoprecipitates from spent media were analyzed by TOF MS as described in materials

Figure 9. MS analysis of immunoprecipitated PCSK9-propeptide from the media of transfected HuH7 cells overexpressing V5-tagged PCSK9 variants. (A–C) TOF-MS analyses of the propeptide of V5-tagged PCSK9 variants as labeled from the media of transfected and overexpressing HuH7 cells. For each variant the change in molecular mass due to the specific amino acid change is show as ΔDa. (D) A graphic representation of the data incorporating results from analyses of the propeptide of V5-tagged wild-type PCSK9. The ratio of unmodified (UM; white bar) or sulfated (SO_4^{2-}; gray bars) to sulfated and phosphorylated (PO_4^{2-}; black bars), calculated as area under the peak as described in materials and methods, is shown ± SE. t-Tests were carried out to compare significant changes in phosphorylation of the propeptide of PCSK9 between variants. Analyses were conducted on at least three independent experiments. ns, nonspecific; *P < 0.05; **P < 0.005; ***P < 0.0005.

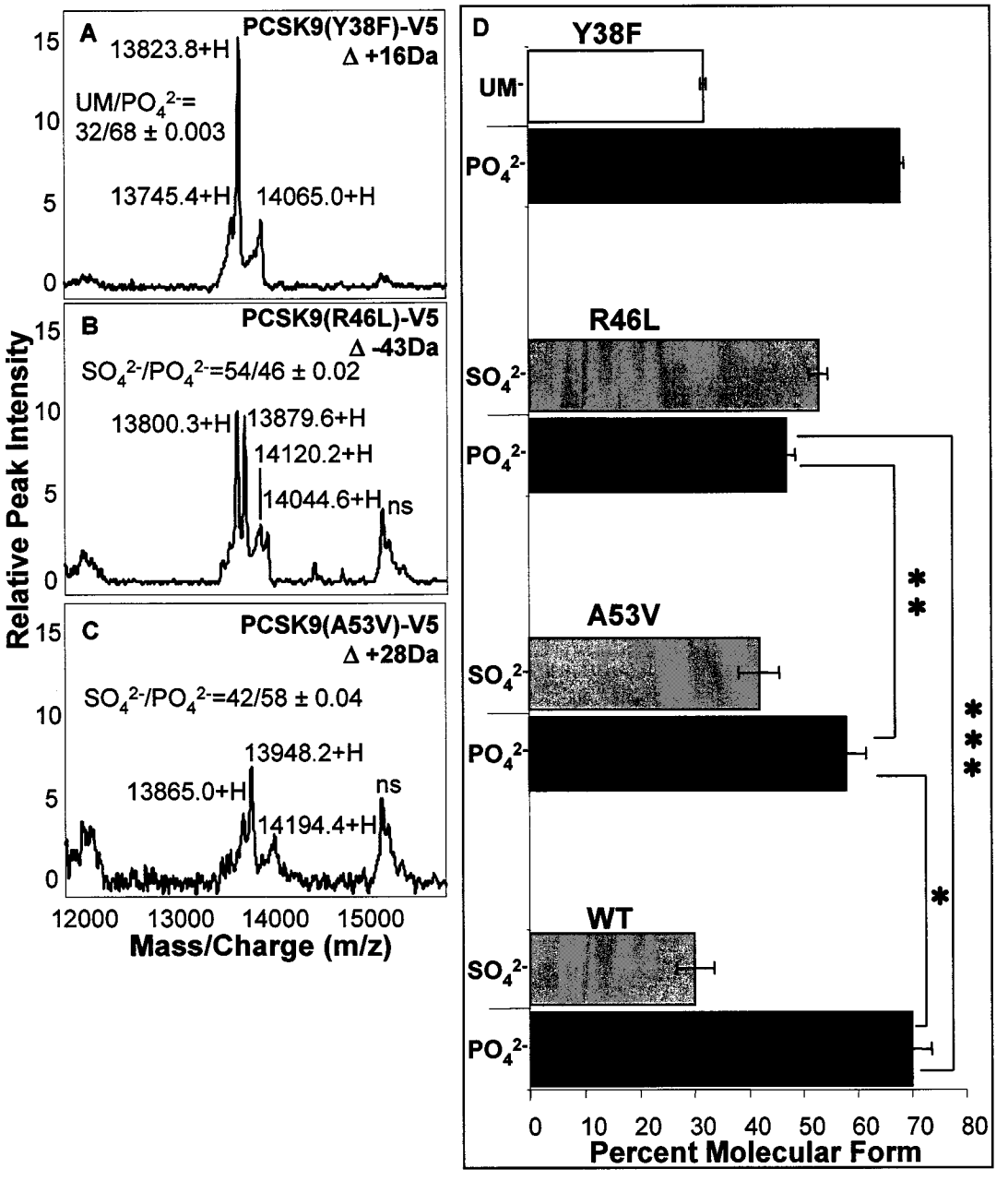
A
PCSK9(Y38F)-V5
Δ +16Da
13823.8+H
UM/PO4 2-=
32/68 ± 0.003
13745.4+H
14065.0+H
B
PCSK9(R46L)-V5
Δ -43Da
SO4 2-/PO4 2-=54/46 ± 0.02
13800.3+H
13879.6+H
14120.2+H
14044.6+H
ns
C
PCSK9(A53V)-V5
Δ +28Da
SO4 2-/PO4 2-=42/58 ± 0.04
13948.2+H
13865.0+H
ns
14194.4+H
Relative Peak Intensity
Mass/Charge (m/z)
D
Y38F
UM-
PO4 2-
R46L
SO4 2-
A53V
WT
Percent Molecular Form

and methods. Ciphergen 3.0 software was used to analyse the area under the peak to compare the ratio of unphosphorylated to phosphorylated PCSK9 propeptide for hPCSK9(Y38F)-V5 as described in materials and methods (Figure 9). Compared to hPCSK9(WT)-V5, only a single peak 80Da greater than unmodified PCSK9 propeptide (13 745.4 Da) was observed in the propeptide of hPCSK9(Y38F)-V5 at 13 823.8 Da, indicating that preventing propeptide sulfation (hPCSK9(Y38F)-V5) did not significantly affect phosphorylation relative to hPCSK9(WT)-V5.

3.3 Identifying Site of PCSK9 C-terminal Phosphorylation and Critical Residues

3.3.1 Identifying Site of PCSK9 C-terminal Phosphorylation.

After identifying the site of phosphorylation in the PCSK9 prodomain, we examined the rest of the amino acid sequence of PCSK9 for other potential sites of phosphorylation with similar consensus motifs. Several potential sites were identified which could be phosphorylated by either GCK-like kinase or CKII (Figure 10). During my Honours Thesis, I studied sterol regulation of PCSK9. I carried out immunoblotting of intracellular and secreted PCSK9 from different cell lines [86]. Several in-house and commercially available PCSK9 antibodies were tested to carry out my studies. A C-terminal PCSK9 antibody from Imgenex, exhibited an interesting difference in detection efficiency between intracellular and extracellular PCSK9. Both proPCSK9 and processed PCSK9 were detectable from intracellular total cell lysates, but it could not detect secreted PCSK9. This suggested that there was either a PCSK9 modification or truncation between intracellular and secreted molecular forms of PCSK9 that the antibody discriminated against, since it recognizes a C-

Figure 10. Amino Acid Sequence of Human PCSK9 Depicting Other Possible Sites of Phosphorylation. Highlighted are other potential sites of phosphorylation in human PCSK9 amino acid sequence based on reported consensus motifs for Protein Kinase CK2 (Casein Kinase II, SXXD/E), Golgi Casein Kinase (GCK, SXE) and a third family member, Protein Kinase CK1 (Casein Kinase I, SXXS). Underlined is the epitope recognized by Imgenex PCSK9 Ab.

MGTVSSRRSWWPLPLLLLLLLLGPAGARAQEDEDGDYEELVLALR**S**EEDGLAEAPEH
GTTATFHRCAKDPWRLPGTYVVVLKEETHL**S**QSERTARRLQAQAARRGYLTKILHVFH
GLLPGFLVKMSGDLLELALKLPHVDYIEEDSSVFAQSIPWNLERITPPRYRADEYQPPD
GG**S**LVEVYLLDT**S**IQSDHREIEGRVMVTDFENVPEEDGTRFHRQA**S**KCDSHGTHLAG
VV**S**GRDAGVAKGA**S**MRSLRVLNCQGKGTVSGTLIGLEFIRKSQLVQPVGPLVVLLPLA
GGYSRVLNAACQRLARAGVVLVTAAGNFRDDACLY**S**PASAPEVITVGATNAQDQPVTL
GTLGTNFGRCVDLFAPGEDIIGAS**S**DCSTCFVSQ**S**GTSQAAAHVAGIAAMML**S**AEPEL
TLAELRQRLIHF**S**AKDVINEAWFPEDQRVLTPNLVAALPPSTHGAGWQLFCRTVW**S**AH
SGPTRMATAVARCAPDEELL**S**CSSFSRSGKRRGERMEAQGGKLVCRAHNAFGGEGV
YAIARCCLLPQANCSVHTAPPAEASMGTRVHCHQQGHVLTGCSSHWEVEDLGTHKPP
VLRPRGQPNQCVGHREASIHASCCHAPGLECKVKEHGIPAPQEQVTVACEEGWTLTG
CSALPGTSHVLGAYAVDNTCVVRSRDVSTTGSTSEGAVTAVAIC<u>CRSRHLAQA**S**QELQ</u>

■ Protein Kinase CKI site ■ Protein Kinase CKII site ■ Golgi Casein Kinase site —— Epitope for Imgenex PCSK9 Antibody

terminal epitope (C679RSRHLAQASQELQ692). Examination of the C-terminal epitope revealed a potential phosphorylation motif at S688QE in PCSK9, similar to the S-X-E motif identified in the propeptide (Figure 10). As a test, immunoprecipitates, using anti-PCSK9 Ab, of secreted PCSK9 from HepG2 cells were treated in the absence or presence of increasing amounts of SAP (1 and 10 U as described in materials and methods), fractionated by SDS-PAGE, electroblotted onto nitrocellulose and immunoblotted with anti-Imgenex PCSK9 Ab as described in materials and methods (Figure 11A, lanes 2-4). PCSK9 was not detected in untreated immunoprecipitates, however PCSK9 was detected with Imgenex PCSK9 Ab upon treatment with 1 U SAP and 10 U SAP. This indicated that the C-terminal Domain of PCSK9 was phosphorylated, and that phosphorylation interferes with Imgenex antibody recognition.

Our group and others commonly tag proteins of interest that are overexpressed in cell biology studies, such as V5 tag [32, 49, 90, 92, 103]. Tagging proteins generally allows for easier manipulation and detection of protein of interest in various cell biology assays. Interestingly, when spent media of HepG2 cells transfected with WT-hPCSK9-V5 was probed using Imgenex PCSK9 Ab, this antibody detected PCSK9 in the absence of SAP (Figure 11A, lane 1). Since the V5-tag is a C-terminal addition, and the epitope for Imgenex PCSK9 Ab is found at the very C-terminus, it is possible that the addition of the V5-tag may disrupt the phosphorylation site in the C-terminus of PCSK9.

The small size shift of the C-terminal PCSK9 corresponding with a loss of phosphorylation could not be accurately detected by TOF MS. The addition of glycosylation and the larger size of the mature PCSK9 (~64kDa) cause a broader peak range (~1-2000 Da) that does not

Figure 11. The prodomain and mature PCSK9 are secreted as phosphoproteins *in vitro*. (A) Immunoprecipitation of overexpressed V5-labeled PCSK9 (lane 1) or endogenous PCSK9 (lanes 2–4) from the media of HepG2 cells followed by dephosphorylation of immunoprecipitates (lanes 3 and 4) and immunoblotting analyses with the anti-hPCSK9 C-terminal Ab (Imgenex). (B) HepG2 and HuH7 cells untransfected (UT; lanes 2, 4 and 6) and transfected with the expression vector for either untagged (lane 7) or V5-tagged hPCSK9 (lanes 1, 3 and 5) were radiolabeled with ^{32}P-orthophosphate as described in materials and methods. Total cell lysates and media were immunoprecipitated with anti-hPCSK9 Ab or anti-V5 Ab conjugated agarose beads and fractionated by SDS- PAGE for phosphorimaging as described in materials and methods. Lane 5 represents the post-immunoprecipitation of endogenously labeled protein following a primary immunoprecipitation for overexpressed V5-tagged protein. The positions of PCSK9, propeptide and alternate propeptide signal peptidase cleavage product (ACS) are noted. Quantitation of the ratio of phosphorylation for propeptide to PCSK9 is shown below each lane. Analyses were conducted on at least three independent experiments.

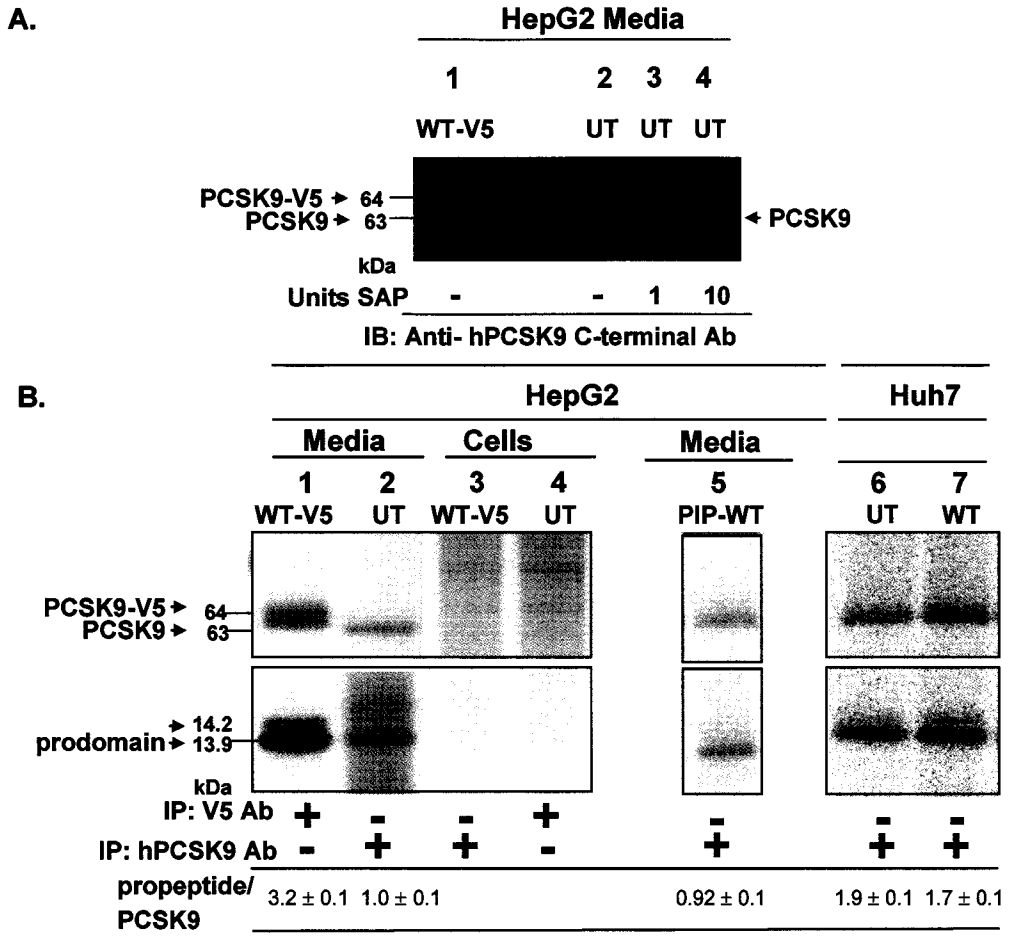
A.
HepG2 Media
1 2 3 4
WT-V5 UT UT UT
PCSK9-V5 64
PCSK9 63
PCSK9
kDa
Units SAP - - 1 10
IB: Anti- hPCSK9 C-terminal Ab
B.
HepG2
Huh7
Media
Cells
Media
1 2 3 4 5 6 7
WT-V5 UT WT-V5 UT PIP-WT UT WT
PCSK9-V5 64
PCSK9 63
14.2
prodomain 13.9
kDa
IP: V5 Ab + - - + - - -
IP: hPCSK9 Ab - + + - + + +
propeptide/ PCSK9
3.2 ± 0.1 1.0 ± 0.1 0.92 ± 0.1 1.9 ± 0.1 1.7 ± 0.1

allow for differentiating between molecular forms of PCSK9 that could differ by only 80Da. As a result, ^{32}P-orthophosphate metabolic labeling was utilized to observe phosphorylation of PCSK9. hPCSK9(WT)-V5 was transiently transfected into HepG2 cells, WT-PCSK9 without a c-terminal tag (hPCSK9(WT)-no tag, in pIRES vector, kindly provided by N.G. Seidah) was transiently transfected into HuH7 cells, and cells were labeled with either ^{32}P-orthophosphate (to detect for phosphorylation) or ^{35}S- Met/Cys (to detect for total protein)as described in materials and methods. Total cell lysates, as well as spent media were immunoprecipitated for PCSK9 using either anti-V5 Ab or anti-hPCSK9 Ab, immunoprecipitates subsequently fractionated by 12% SDS-PAGE, dried down under vacuum and visualized using Typhoon Storage Phosphor Imager as described in materials and methods (Figure 11B). Both phosphorylated PCSK9 and its propeptide were detected in spent media immunoprecipitates of transfected and untransfected HepG2 cells, since HepG2 express phosphorylated PCSK9 endogenously (Figure 11B, lane 1 and 2). No phosphorylated PCSK9 or propeptide were detected intracellularly however (Figure 11B lane 3 and 4). The ratio of propeptide to C-terminal PCSK9 was 1:1 in untransfected cells, but was 3-fold higher with overexpressed WT-hPCSK9-V5. In contrast, for HuH7 transfected and untransfected cells, the ratio of propeptide to C-terminal PCSK9 was ~2:1 between overexpressed WT-hPCSK9-no tag and endogenous PCSK9 (Figure 11B lane 6 and 7). Spent media of WT-hPCSK9-V5 from HepG2 was immunoprecipitated subsequently with anti-PCSK9 Ab to determine whether the difference observed in ratio of propeptide to C-terminal PCSK9 between transfected and untransfected HepG2 cells was due to saturation. This post-IP revealed endogenous PCSK9, phosphorylated at same ratio as PCSK9 from untransfected HepG2 cells (kinase was not saturated during overexpression) (Figure 11B lane 5). Collectively, this suggested that in the C-terminus of V5-tagged WT-hPCSK9, C-

terminal phosphorylation may be disrupted, supporting our earlier results with Imgenex PCSK9 Ab.

This potential phosphorylation site (S688QE) identified in the C-terminal domain of PCSK9 conformed to a GCK consensus motif similar to the site identified in the PCSK9 propeptide. Constructs (using hPCSK9(WT)-no tag as a template) of the potential phosphoserine S688A, and its P+2 residue E690A, were engineered by SDM to determine whether C-terminal phosphorylation could be prevented (as described in materials and methods). ^{32}P-orthophosphate metabolic labeling was utilized to observe phosphorylation of PCSK9. The mutant constructs were transiently transfected into HuH7 cells and labeled with either ^{32}P-orthophosphate (to detect for phosphorylation), or ^{35}S-Met/Cys (to detect for total protein) as described in materials and methods. Total cell lysates as well as spent media were immunoprecipitated using anti-PCSK9 Ab, immunoprecipitates subsequently fractionated through 12% SDS-PAGE, dried down under vacuum and visualized using Typhoon Storage Phosphor Imager as described in materials and methods. Compared to control untransfected HuH7, as assessed by ^{35}S- Met/Cys labeling, transient transfections expressed ~3.5x more PCSK9 protein (both PCSK9 and propeptide) (Figure 12A, B). Phosphorylation of PCSK9 prodomain was unaffected (again transient transfections expressed ~3.5x more phosphorylated PCSK9 than control), while only endogenous levels of PCSK9 were visualized in C-terminal PCSK9 (~0.81-1). This demonstrated that Ser688 was the C-terminal phosphoserine, and that Glu690 was a critical residue for C-terminal phosphorylation, suggesting that a golgi casein kinase-like kinase phosphorylates both major phosphosites identified.

Figure 12. Site-Directed Mutagenesis of the C-terminal phosphorylation region of PCSK9. *A* and *B*, HuH7 cells untransfected (lanes 2 and 4; endogenous- C) and transfected with cDNAs encoding untagged PCSK9 C-terminal variants (lane 1 and 3 and 5–8 as labeled) were radiolabeled with either ^{35}S- Cys/Met (lanes 1–3) or ^{32}P-orthophosphate (lanes 4–8) as described in materials and methods. Media was immunoprecipitated with anti-hPCSK9 IgG, fractionated by SDS -PAGE for phosphorimaging as described in materials and methods. The positions of PCSK9, propeptide and alternate propeptide signal peptidase cleavage product (ACS) are noted. Quantitation of the ratio of total protein immunoprecipitated (setting untranfected endogenous-C as 1) is shown below each lane. *C*, HuH7 cells untransfected and transfected with cDNA encoding PCSK9(S47A/S688A) variant were radiolabeled with either ^{35}S- Cys /Met or ^{32}P-orthophosphate as described in materials and methods. Media were immunoprecipitated with anti-hPCSK9 Ab, fractionated by SDS -PAGE for phosphorimaging as described in materials and methods. The positions of PCSK9 and propeptide are noted. Quantitation of the ratio of total protein immunoprecipitated (setting untranfected endogenous-C as 1) is shown below each lane.

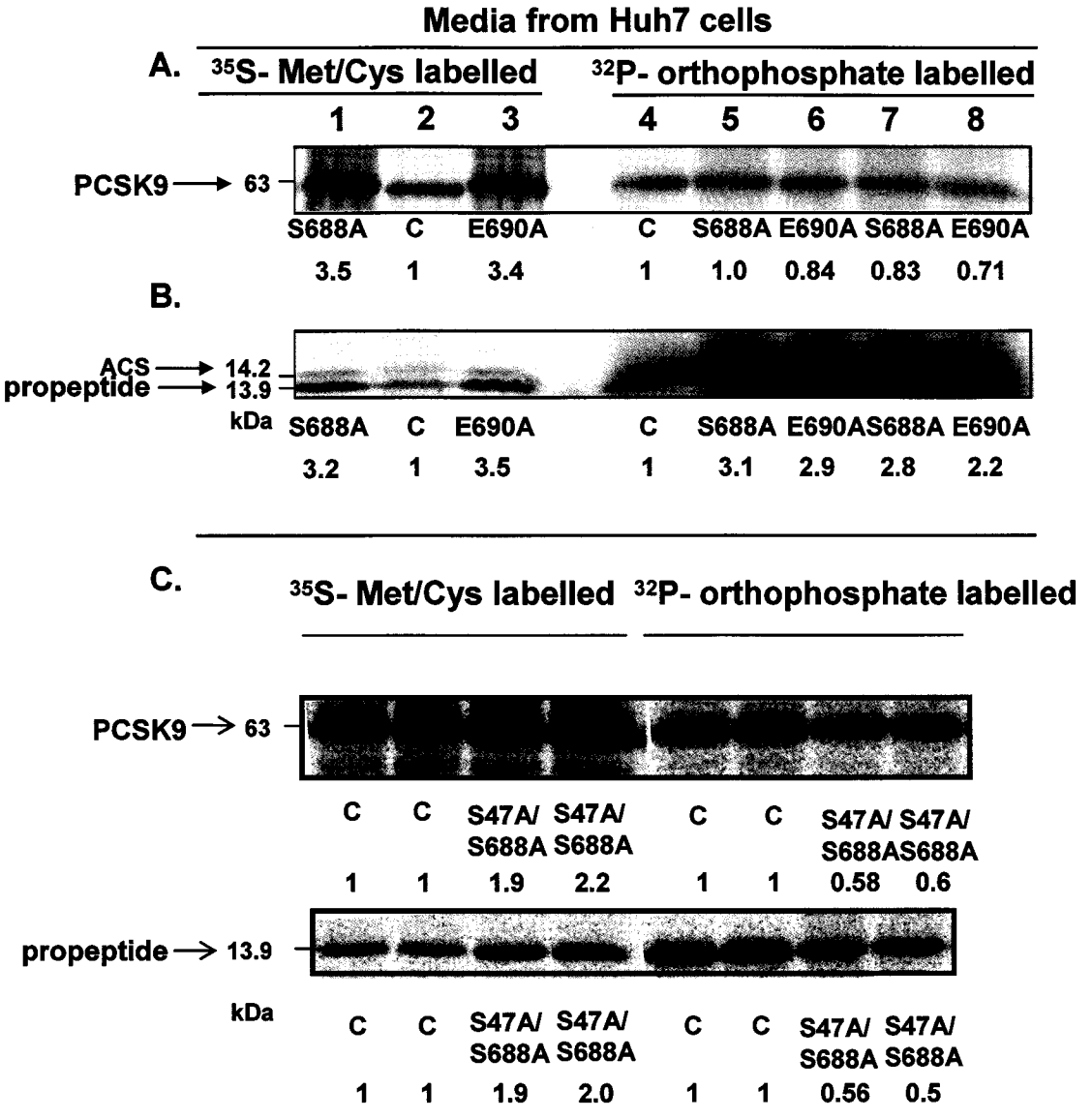
Media from Huh7 cells
A.
35S- Met/Cys labelled
32P- orthophosphate labelled
1 2 3 4 5 6 7 8
PCSK9 → 63
S688A C E690A C S688A E690A S688A E690A
3.5 1 3.4 1 1.0 0.84 0.83 0.71
B.
ACS → 14.2
propeptide → 13.9
kDa
S688A C E690A C S688A E690A S688A E690A
3.2 1 3.5 1 3.1 2.9 2.8 2.2
C.
35S- Met/Cys labelled
32P- orthophosphate labelled
PCSK9 → 63
C C S47A/S688A S47A/S688A C C S47A/S688A S47A/S688A
1 1 1.9 2.2 1 1 0.58 0.6
propeptide → 13.9
kDa
C C S47A/S688A S47A/S688A C C S47A/S688A S47A/S688A
1 1 1.9 2.0 1 1 0.56 0.5

A mutant with a substitution of alanine at both identified phosphoserines was engineered by SDM, hPCSK9(S47A/S688A)-no tag. Either untransfected or this mutant construct were transiently transfected into HuH7 cells and labeled with either ^{32}P-orthophosphate (to detect for phosphorylation), or ^{35}S-Met/Cys (to detect for total protein) as described in materials and methods. Spent media were immunoprecipitated using anti-PCSK9 Ab, immunoprecipitates subsequently fractionated through 12% SDS-PAGE, dried down under vacuum and visualized using Typhoon Storage Phosphor Imager as described in materials and methods (Figure 12C). Compared to control untransfected HuH7, as assessed by ^{35}S-Met/Cys labeling, transiently transfected cells expressed ~2x more PCSK9 protein (both PCSK9 and propeptide), while level of phosphorylation visualized for PCSK9 and its propeptide was comparable to endogenous levels of PCSK9 (Figure 12 C). This indicated that in this cell line, PCSK9 is only phosphorylated at Ser47 and Ser688, since overexpressed phosphorylated PCSK9 was not detected with this double mutant.

3.4 PCSK9 Phosphorylation in Processing

3.4.1 Processing of PCSK9 Phospho-mutants

Phosphorylation can affect among other things subcellular localization and secretion of proteins [126]. PCSK9 mediates LDLR degradation prominently through the extracellular pathway, whereby secreted PCSK9 binds LDLR, and redirects the complex from the endosomal recycling pathway to the lysosome for degradation. If phosphorylation of PCSK9 affects its rate of secretion and therefore extracellular availability, this may contribute to a

'loss of function' phenotype. We determined whether altering phosphorylation status might affect the rate of secretion of PCSK9. If our PCSK9 phosphomutants are poorly secreted, there should be increased retention of these mutants intracellularly, compared to hPCSK9(WT).

PCSK9 mutants were engineered which either prevent or mimick phosphorylation at either N-terminal or C-terminal site of phosphorylation individually or in combination (Phospho-null or phospho-mimick, respectively as described in materials and methods (Table 2). ^{35}S-Met/Cys metabolic labeling was used to label total protein from transient transfections of these engineered mutants in HuH7 cells, to assess whether rate of secretion of these mutants was affected as described in materials and methods. 48 hours after transient transfection, a 3.5 hour pulse with ^{35}S -Met/Cys was conducted, and total cell lysates as well as spent media were immunoprecipitated with anti-hPCSK9 Ab. Immunoprecipitates were fractionated through 12% SDS-PAGE, dried down under vacuum and visualized using Typhoon Storage Phosphor Imager as described in materials and methods. Comparing the ratio of total intracellular PCSK9 (that is proPCSK9 and intracellular PCSK9) to total extracellular PCSK9 (that is secreted full length PCSK9 and its Furin-cleaved form) no significant change was detected between PCSK9 phosphomutants compared to hPCSK9(WT) (Figure 13A). The ratio of secreted PCSK9 to its secreted cleaved form was not significantly different either (Figure 13B). Collectively these results show that the phosphorylation status of PCSK9 and its propeptide did not affect its secretion nor the conversion of secreted PCSK9 to its inactive furin-cleaved form.

Figure 13. Pulse-Labelling to Assess Differences in Processing of PCSK9 Phospho-mutants. HuH7 cells transfected with cDNAs encoding untagged PCSK9 variants WT S47A, S47E, S688A, S688E, S47A/S688A, S47E/S688E (see materials and methods). After 48 hrs total cell lysates and total media were immunoprecipitated with in-house anti-hPCSK9 Ab overnight and fractionated by 12% SDS-PAGE. PCSK9 was visualized using Typhoon 8600 Variable Mode Storage Phosphor Imager. *A*, Ratio of total intracellular PCSK9/total secreted PCSK9 for all mutants described above. *B*, Ratio of full length secreted PCSK9/the secreted furin-cleaved PCSK9 for all mutants described above. Data represents mean ± SEM (n=4).

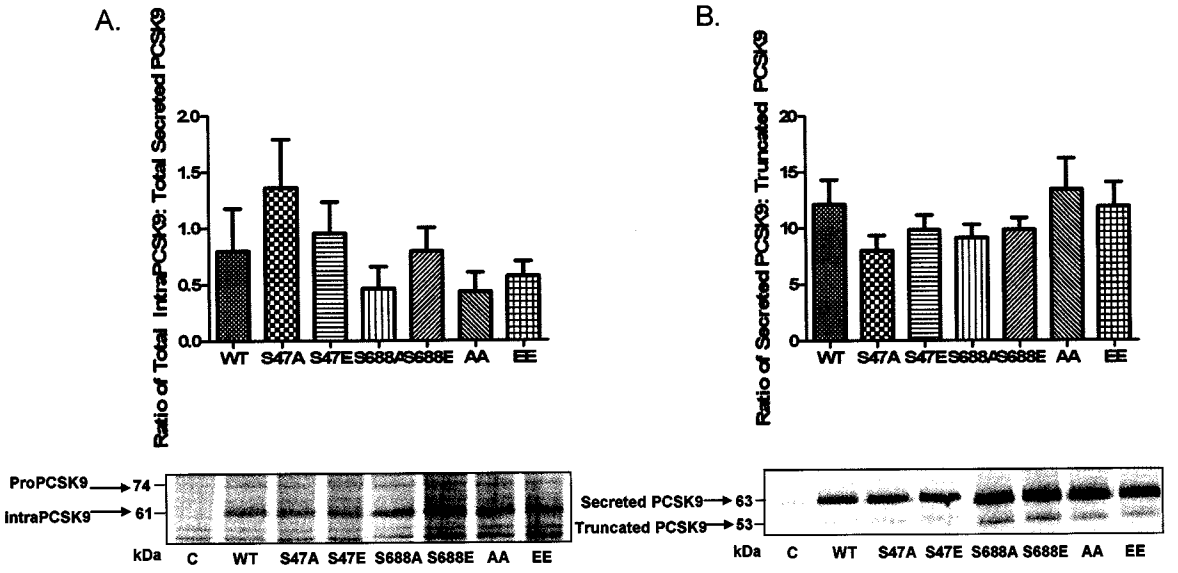
A.
Ratio of Total IntraPCSK9: Total Secreted PCSK9
2.0
1.5
1.0
0.5
0.0
WT S47A S47E S688A S688E AA EE
B.
Ratio of Secreted PCSK9: Truncated PCSK9
20
15
10
5
0
WT S47A S47E S688A S688E AA EE
ProPCSK9 → 74
IntraPCSK9 → 61
kDa C WT S47A S47E S688A S688E AA EE
Secreted PCSK9 → 63
Truncated PCSK9 → 53
kDa C WT S47A S47E S688A S688E AA EE

3.4.2 Stability of PCSK9 Phosphomutants

During our TOF MS analyses of the molecular forms of the PCSK9 propeptide generated by mutagenesis of the sites surrounding Ser47 phosphorylation (Figure 8), a fragment of lower molecular mass, 11 738.2 Da for PCSK9(E49A) propeptide and 11782.8 for PCSK9(R46L) propeptide was observed in the media of HuH7 cells transfected with these phosphomutants that was not found in those transfected with hPCSK9(WT) (Figure 14A insert).

This fragment accounted for 13% and 5% of the total propeptide molecular forms for the PCSK9(E49A)-V5 and PCSK9(R46L)-V5 mutants, respectively, as assessed by calculating areas under the peak, but was not detected in the spectrum of the propeptide from PCSK9(WT)-V5 (Figure 14A insert). This fragment corresponds to cleavage of the propeptide following Ser47 (observed molecular mass Q31-Ser47 2026.1 Da versus calculated 2044.1 Da for E49A mutant and observed 2000.1 Da versus calculated 2001.1 Da for R46L mutant) (Figure 14A insert). Calculated molecular masses were determined using Client Paws software. In ^{35}S-Met/Cys metabolic labeling studies carried out as described in the previous section, this fragment was also visualized in immunoprecipitates of spent media from HuH7 cells transiently transfected with hPCSK9(E49A)-no tag, where this fragment accounted for ~10% of the total propeptide (Figure 14C). Phosphorylation is capable of altering stability of proteins and their resistance to proteolysis by disrupting recognition motifs of proteases [135]. Phosphorylation in the propeptide of PCSK9 may protect it against proteases which would otherwise cleave the propeptide, suggesting phosphorylating PCSK9 may prolonged its half-life compared to unphosphorylated PCSK9.

Figure 14. Phosphorylation of PCSK9 Propeptide Affects Its Stability. *A*, TOF-MS analyses of the propeptide of V5-tagged PCSK9 variants as labeled from the media of transfected and overexpressing HuH7 cells. Insets highlight the presence or absence of proteolysis fragments of the parent propeptide. *B*, Amino acid sequence of PCSK9 propeptide proteolytic fragment corresponds to cleavage after Ser47. *C*, HuH7 cells transiently transfected with hPCSK9(WT) or hPCSK9(E49A) (see materials and methods). After 48 hrs HuH7 cells were starved in Cys /Met-free DMEM for 30min, and incubated in 350 μCi of ^{35}S- Cys /Met for 3.5 hours. Total cell lysates and total media were immunoprecipitated with in-house PCSK9 Ab for 48hrs and fractionated by 12% SDS-PAGE. PCSK9 was visualized using Typhoon 8600 Variable Mode Storage Phosphor Imager. The positions of propeptide, alternate propeptide signal peptidase cleavage product (ACS), and truncated cleavage product are noted.

A.

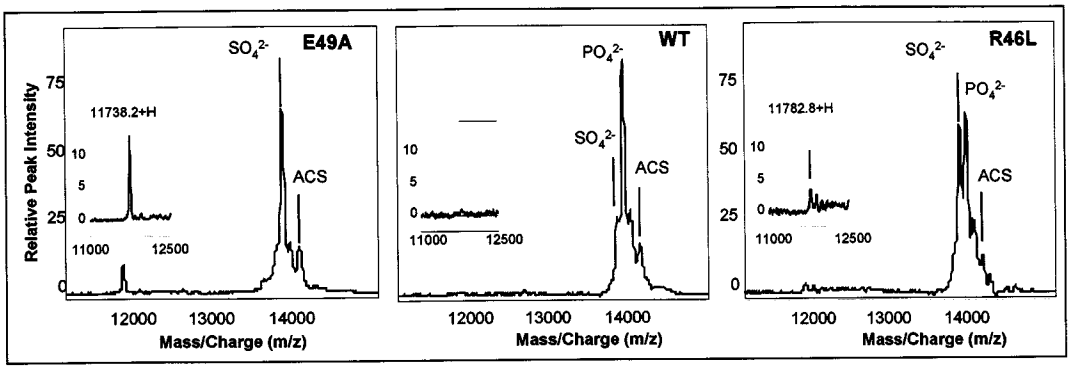

B.

Q31EDEDGDY[SO_4^{2-}]EELVLALRSEEDGLAEAPEHGTTATFHR66
CAKDPWRLPGTYVVVLKEETHLSQSERTARRLQAQAARRGYLTKILHV
FHGLLPGFLVKMSGDLLEALKLPHVDYIEEDSSVFAQ152

C.

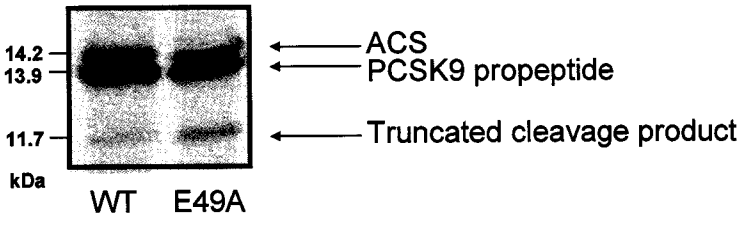

3.5 Functional Assay of PCSK9 Phosphorylation

3.5.1 Effect of Phospho-null PCSK9 mutants on LDLR Degradation

The only known physiological function of PCSK9 is to promote the degradation of the LDLR [32, 49, 50]. To accomplish this PCSK9 interacts with LDLR as a chaperone, binding at its EGF-A domain, which leads to subsequent internalization of this complex and translocation to the lysosome for degradation. We have observed that the hypocholesterolemic PCSK9 variant R46L is hypophosphorylated and that its prodomain is susceptible to proteolyses (Figure 14A), while others have observed that this variant binds less to LDLR, potentially explaining its mechanism of action [136]. To determine whether phosphorylation of PCSK9 or its propeptide affected its ability to promote LDLR degradation, we used SDM to generate vectors for expression of PCSK9 mutated at the propeptide and C-terminal sites of phosphorylation. These vectors were transiently transfected into HuH7 cells (Table 2). Total cell lysates were fractionated by SDS-PAGE and immunoblotted as described in materials and methods, to compare the level of LDLR degradation between different PCSK9 mutants and hPCSK9(WT).

PCSK9 mutants were engineered which prevent phosphorylation at either N-terminal or C-terminal sites of phosphorylation individually or in combination (Table 2). Since the addition of a C-terminal V5-tag disrupted C-terminal phosphorylation, these new constructs were engineered using hPCSK9(WT) without C-terminal tag (hPCSK9(WT)-no tag) as a template as described in materials and methods. Phospho-null PCSK9 mutants S47A-, E49A-, S688A-, E690A- (Figure 15A) and S47A/S688A-PCSK9 (Figure 15C) were transiently transfected

into HuH7 cells, and after 72hrs incubation, total cell lysates and spent media were collected. 50μg of total cell lysate were fractionated through 10% SDS-PAGE, transferred to nitrocellulose and analyzed by immunoblotting for changes in LDLR levels using a commercial LDLR Ab, with transferrin receptor as a loading control (transferrin receptor is commonly used in the literature as a loading control as this receptor has not been shown to be affected by changes in PCSK9), as described in materials and methods. The level of LDLR in HuH7 cells expressing different mutants which prevent phosphorylation is displayed in Figure 15 panel A, and C. Levels of LDLR are relative to untransfected control HuH7 cells. No significant difference in the level of PCSK9 expression was observed between transfections of different phosphomutants and wild-type (data not shown), therefore any changes in LDLR levels are due to a modification in PCSK9 function towards LDLR and not due to overall changes in secreted PCSK9 levels. Relative to hPCSK9(WT), all single phospho-null PCSK9 mutants significantly reduced LDLR degradation (Figure 15A). Unlike the single phospho-null mutations of either the PCSK9 propeptide (S47A) or C-terminal PCSK9 (S688A), the double phospho-null mutant PCSK9(S47A/S688A) showed increased levels of LDLR levels relative to PCSK9(WT), that did not reach significance ($p=0.11$). As a positive control, hPCSK9 (D374Y), which acts by binding LDLR 10x stronger than hPCSK9(WT), increased LDLR degradation greater than hPCSK9(WT) as expected (Figure 15A). The 'loss of function' phenotype observed in the absence of PCSK9 phosphorylation suggests that phosphorylation of PCSK9 may convey a 'gain of function' against LDLR.

Figure 15. HuH7 cells transiently expressing PCSK9 phospho-mutants modulate LDLR levels. *A*, Relative intensity of LDLR levels in HuH7 cells transiently expressing PCSK9 phosphonull mutants relative to wildtype. HuH7 cells transfected with WT- PCSK9, N-terminal and C-terminal PCSK9 phosphonull mutants S47A, E49A, S688A, and E690A, for 72 hrs as described in materials and methods. Total cell lysates were fractionated by SDS-PAGE, and analysed by immunoblotting as described in materials and methods. LDLR was detected with commercial LDLR Ab (Fitzgerald) and corrected against loading control transferrin receptor (monoclonal Ab, Invitrogen). PCSK9(D374Y) was used as a positive control. *B*, Relative intensity of LDLR levels in HuH7 cells transiently expressing PCSK9 phosphomimick mutants, relative to wildtype. HuH7 cells transfected with N-terminal and C-terminal PCSK9 phosphomimick mutants S47D, S47E, E49D, S688D, S688E, and E690D following same protocol as A. *C*, Relative intensity of LDLR levels in HuH7 cells transiently expressing PCSK9 double phosphomutants, relative to wildtype. HuH7 cells transfected with PCSK9 double mutants S47A/S688A, S47D/S688D, and S47E/S688E following same protocol as *A*. Data represents mean + SEM (n>3).

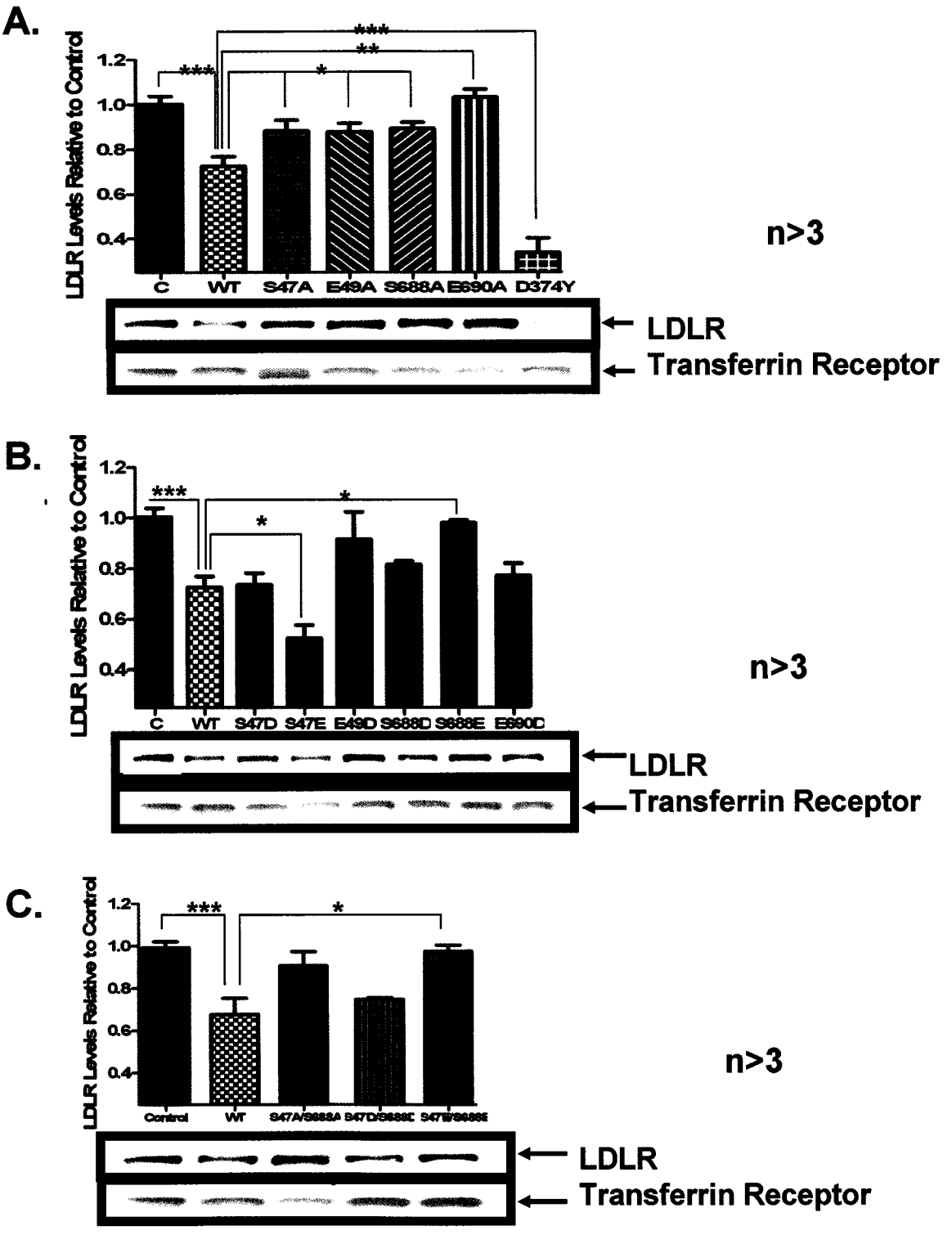
A.
LDLR Levels Relative to Control
1.2
1.0
0.8
0.6
0.4
***
**
*
***
C
WT
S47A
E49A
S688A
E690A
D374Y
LDLR
Transferrin Receptor
n>3
B.
LDLR Levels Relative to Control
1.2
1.0
0.8
0.6
0.4
***
*
*
C
WT
S47D
S47E
E49D
S688D
S688E
E690D
LDLR
Transferrin Receptor
n>3
C.
LDLR Levels Relative to Control
1.2
1.0
0.8
0.6
0.4
***
*
Control
WT
LDLR
Transferrin Receptor
n>3

3.5.2 Effect of Phospho-mimicking PCSK9 mutants on LDLR Degradation

It has been reported in the literature that substituting a phospho-receptive amino acid for either glutamic acid or aspartic acid can sometimes mimic phosphorylation, with their size and negative charge [137]. PCSK9 mutants were engineered by SDM which might mimick PCSK9 phosphorylation (Phospho-mimick), to determine their effect on LDLR degradation (Table 2). Phospho-mimicking PCSK9 mutants were transiently transfected into HuH7 cells, and after 72hrs incubation, total cell lysates and spent media were collected and analysed as in previous section.

The phospho-micking mutant hPCSK9(S47D) in PCSK9 propeptide behaved similarly to hPCSK9(WT) in terms of LDLR degradation while the phospho-mimicking mutant, hPCSK9(S47E), resulted in increased LDLR degradation (Figure 15B). The remaining N-terminal mutant, hPCSK9(E49D), substituted at the critical P+2 position, did not increase LDLR degradation (Figure 15B). This result is not unexpected as this mutant was shown to be secreted in its sulfated form earlier (Figure 8E). At the C-terminus of PCSK9, neither Asp substituted PCSK9 phospho-mimick mutant had a significant effect on LDLR levels in comparison to cells transfected with hPCSK9(WT) (Figure 15B). Interestingly, hPCSK9(S688E) resulted in a significant reduction in LDLR degradation comparison to cells transfected with hPCSK9(WT) (Figure 15B). These results suggest that mimicking phosphorylation at the PCSK9 propeptide, especially with Glu, is capable of affecting PCSK9-mediated LDLR degradation, while at the C-terminus of PCSK9, this was not the case.

The doubly mimicking mutant hPCSK9(S47D/S688D) behaved similarly to hPCSK9(WT) in terms of LDLR degradation (Figure 15C) and as had been observed for single mutants at either site (Figure 15B). Transfection of the double mimicking mutant hPCSK9(S47E/S688E) (Figure 15C) affected LDLR levels similar to those observed with the single PCSK9 C-terminal phospho-mimicking mutant hPCSK9(S688E) (Figure 15B), significantly reducing LDLR degradation but unlike its single propeptide phospho-mimicking mutant hPCSK9(S47E) (Figure 15B). This suggests that an amino acid substitution that maintains size/charge of phosphorylation in the N-terminus can maintain PCSK9 gain-of-function, while in the C-terminus this substitution alone can not. Also the PCSK9(S47E/S688E) double mutant suggests the importance of the C-terminal domain in PCSK9 function as the effect of the N-terminal Glu substitution on PCSK9-mediated LDLR degradation is prevented by the C-terminal Glu substitution.

3.6 PCSK9 Phosphorylation Status and Annexin A2 Interaction

3.6.1 Effect of Phosphorylation on PCSK9: Annexin A2 Interaction

Mayer and colleagues reported that PCSK9 interacts with a protein other than LDLR found at the cell surface, annexin A2 [103]. They demonstrated that the C-terminal domain of PCSK9 interacted with the N-terminal extracellular domain of annexin A2, and that this interaction provided a competitive inhibition of PCSK9 action against LDLR. With PCSK9 bound to annexin A2, it is unavailable to bind LDLR, which consequently increases LDLR recycling. Phosphorylation affects protein-protein interactions, and we have shown that

PCSK9-mediated LDLR degradation is affected by phosphorylation status (Figure 15). Here we wanted to determine whether phosphorylation status of PCSK9 could affect the interaction between PCSK9 and annexin A2, therefore indirectly affecting LDLR levels.

hPCSK9(WT) (70% phosphorylated in HuH7 cells, Figure 6F), and unphosphorylated hPCSK9(S47A/S688A) were transiently transfected into HuH7 cells, and spent media collected as described in materials and methods. Immunoprecipitations of this media were immunoblotted alongside a standard amount of recombinant PCSK9 protein to determine concentrations of PCSK9 in each spent media as described in materials and methods (Figure 16A). Total cell lysates were collected from three cell lines commonly used to study PCSK9, HuH7 (an annexin A2 positive cell line), HepG2 and HEK293 (both annexin A2 negative cell lines for control).

Immunoblots containing either 100μg of HuH7, HepG2, or HEK293 total cell lysate were incubated with equal amounts of either PCSK9(WT) or PCSK9(S47A/S688A) spent media for 3hrs, following Far Western technique as described in materials and methods. Immunoblots were subsequently probed with anti-PCSK9 Ab as described in materials and methods. Bands were identified in both control cell lines, HepG2 and HEK 293 which were not at the size of annexin A2 (Figure 16B). In HuH7 total cell lysate, hPCSK9(S47A/S688A) bound more strongly than PCSK9(WT) to a protein of ~35kDa corresponding to annexin A2 (confirmed by stripping and reprobing of this blot with anti-annexin A2 Ab (Figure 16C)) (Figure 16B). This suggested that per equal amount of PCSK9 protein, unphosphorylated PCSK9 preferentially interacts with annexin A2 than phosphorylated PCSK9.

Figure 16. Far Western Analysis of Phosphorylation on PCSK9: Annexin A2 Interaction. *A*, Spent media collected from HuH7 cells overexpressing phosphorylated PCSK9(WT) and unphosphorylated PCSK9(S47A/S688A) were immunoprecipitated for in-house anti-PCSK9 Ab, fractionated by 10% SDS-PAGE and immunoblotted for anti-PCSK9 Ab. *B*, 100μg of HuH7, HepG2, and HEK 293 total cell lysates were fractionated by SDS-PAGE and transferred to nitrocellulose. Spent media collected from HuH7 cells over-expressing phosphorylated PCSK9(WT) and unphosphorylated PCSK9(S47A/S688A) were added to the immunoblots for 3hrs and the blots were subsequently probed using in-house anti-PCSK9 AB. *C*, Immunoblot incubated with spent media collected from HuH7 cells over-expressing phosphorylated PCSK9(WT) was stripped and reprobed to confirm annexin A2 alone.

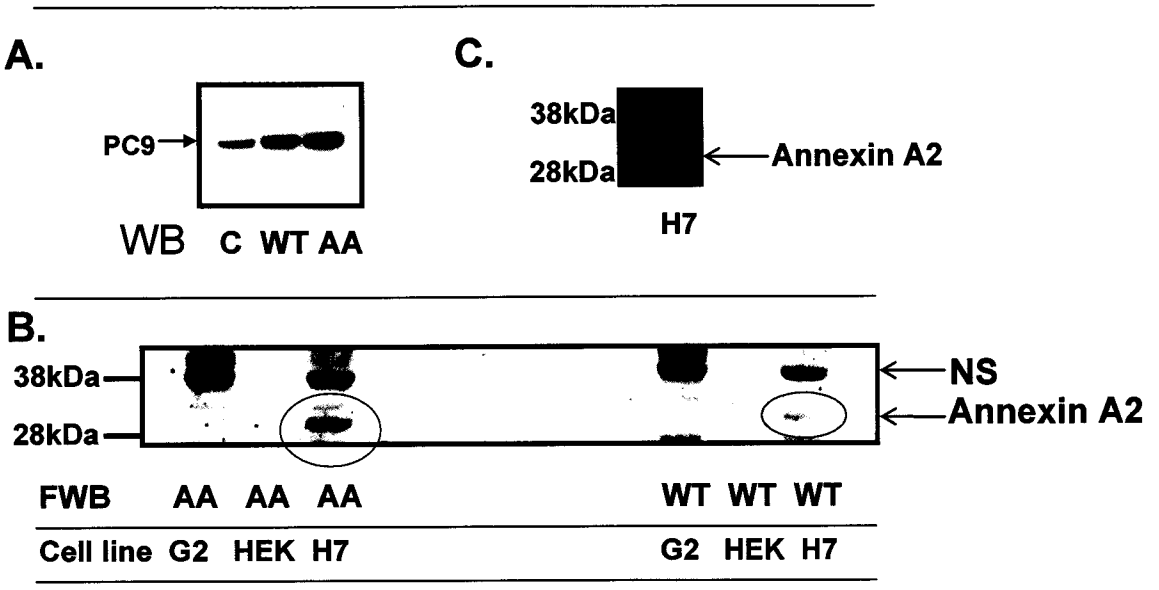
A.
PC9
WB C WT AA
C.
38kDa
28kDa
Annexin A2
H7
B.
38kDa
28kDa
NS
Annexin A2
FWB AA AA AA WT WT WT
Cell line G2 HEK H7 G2 HEK H7

4. Discussion

4.1 PCSK9 Phosphorylation is Cell-Type Specific

As PCSK9 transits through the secretory pathway, post-translational modifications (PTMs) occur. In the ER proPCSK9 is glycosylated at Asn533 in its C-terminal domain [32]. To exit the ER, the 74kDa proPCSK9 autocatalytically cleaves itself at VFAQ↓SIP to a 60kDa form, which along with the PCSK9 propeptide forms a propeptide: PCSK9 heterodimer [12]. The PCSK9 sugar moiety is subsequently matured in the Golgi leading to an approximate increase in size of ~2200 Da, which is why a mobility shift is observed by SDS-PAGE between secreted and intracellular PCSK9 [32]. Our group reported that a sulfation occurs at Tyr38 in the PCSK9 propeptide [89]. This addition likely occurred late in the TGN since sulfated PCSK9 was not detected intracellularly [89]. Here we report that PCSK9 is secreted as a phosphoprotein; PCSK9 is phosphorylated at two sites, Ser47 in the propeptide, and Ser688 in the C-terminus (Figure 5) [90].

PCSK9 and propeptide phosphorylation is cell-type specific as PCSK9 is phosphorylated 70% in HuH7 cells, 55% in HepG2 cells, 23% in HEK 293 cells and is not phosphorylated in CHO K1 cells (Figure 6). Phosphorylation of PCSK9 and its propeptide likely occurs either late in the Golgi prior to secretion or in the extracellular environment, as we have not been able to detect intracellular phosphorylated PCSK9 by either of two commonly used sensitive techniques, MS or radiolabeling (Figure 11B). A difference in the cellular localization and availability of kinase(s) responsible for phosphorylating PCSK9 in these different cell lines could account for this difference observed.

4.2 A Golgi Casein Kinase-like Kinase Phosphorylates PCSK9

PCSK9 is efficiently and rapidly secreted upon its maturation in the secretory pathway since the TGN matured glycosylated, sulfated form of PCSK9 (which can only occur in the Golgi) is not detected intracellularly [89]. Kinases likely to phosphorylate PCSK9 would reside either in the TGN or in the extracellular environment. Members of the acidophilic Casein Kinase class of Ser/Thr kinases have been implicated in mediating the phosphorylation of several secretory proteins, including insulin growth factor-like binding protein, osteopontin, aquaporin, PCSK3/Furin and the PCSK2 chaperone protein 7B2, among others [122, 124-126]. Of this family, two kinases, protein kinase CKII (casein kinase II, S-X-X-D) and Golgi casein kinase (GCK, S-X-E) recognize a consensus motif similar to one surrounding the PCSK9 propeptide phosphoserine, S47EED [131-134]. Through SDM studies the P+2 residue at both the PCSK9 propeptide and C-terminus of PCSK9 was shown to be 100% crucial for serine phosphorylation, suggesting that a GCK-like kinase is likely responsible for phosphorylating both PCSK9 phosphoserines (Figure 8, 12). With the exception of the tamarin monkey, the region at the propeptide phosphorylation site is completely conserved among primates. This region is also conserved in mouse and rat (PSQED for both), and still conforms to a GCK consensus motif [134]. At the C-terminus, the region surrounding Ser688 is completely conserved in 12 of 14 primate species and conforms to a GCK consensus motif, but not conserved at all in either mouse or rat [138].

Relatively little is known about the Golgi casein kinase. Initially identified in the Golgi enriched fractions (GEF-casein kinase) of the lactating mammary glands, this casein kinase

recognizes a sequence motif, mentioned earlier, that is characteristic of phosphorylation sites in casein [134]. This kinase has been difficult to isolate or purify alone, rather it is copurified in a supercomplex which includes potential substrates [139]. As such, currently no crystal structure has been reported. Unlike CK2, which is found in the cytoplasm or at the cell surface, GCK is believed to be specifically localized in the Golgi apparatus. Marina Lasa and colleagues screened for this kinase in other tissue types using a β-casein peptide substrate specific for GCK recognition (but not CK2), identifying a similar kinase in several tissues including brain, spleen, and rat liver Golgi extracts [140]. Studies by Lasa and colleagues also determined the highly stringent nature of the recognized consensus motif for GCK, where only another phosphoserine could partially replace the P+2 Glu residue as a specificity determinant [134]. Subsequent studies with the proline-rich protein (PRP-1) by Brunati and colleagues have since revealed an additional novel recognition motif for GCK, $SXQXX(D/E)_3$ (X is any amino acid), where the acidic residues at P+5 and P+7 are critical determinants [133].

4.3 Domain Characteristics of PCSK9

Phosphorylation is an important post-translational modification capable of augmenting the biological and chemical nature of a protein. The steric size and negative charge of the addition of a phosphoryl group contribute to conformational changes in a protein which can lead to the activation/deactivation of enzymatic activity, promote participation in cellular signal transduction events, alter protein stability, or sub-cellular colocalization, and fundamentally modulate protein-protein interactions [119, 120, 122, 126]. What role does phosphorylation at either site play in PCSK9 structure and function?

The PCSK9 propeptide and C-terminal domain where PCSK9 is phosphorylated, are two peripheral regions that are solvent exposed but do not directly associate with the EGF-A domain of LDLR [96, 98]. Several groups have produced PCSK9 crystal structures, however crystallization of the first 23 amino acids of the prodomain and last 20 amino acids of the C-terminal domain have not been successful due to a lack of electron density in these regions [96, 141]. As a result, descriptions of the prodomain begins at Thr61 downstream of the propeptide site of phosphorylation, and in the C-terminus end at R682 upstream of the C-terminal phosphorylation site [96, 141]. Interestingly, Kwon and colleagues demonstrated that a prodomain truncated recombinant Δ53-hPCSK9 had a stronger affinity for LDLR [96]. This may suggest the N-terminal region of the prodomain, where the propeptide site of phosphorylation is found, may promote a regulatory effect on PCSK9 function.

The C-terminal domain is predicted to be involved in modulating protein-protein interactions among other things. Indeed it is the C-terminal domain of PCSK9 which interacts with the scaffolding protein annexin A2 as recently demonstrated by Mayer and colleagues [103]. Phosphorylation is capable of changing the conformation of proteins, thus affecting protein-protein interactions as well. In our studies we demonstrated that a C-terminal V5-tag on PCSK9 was capable of disrupting and reducing C-terminal phosphorylation of PCSK9 (Figure 11). PCSK9 with a C-terminal tag, either V5 (a 14 amino acid extension) or His (a hexa-his sequence), is commonly used to study binding, and colocalization of PCSK9 with LDLR as well as to produce and purify recombinant PCSK9 for crystal structures studies [96, 98, 103]. Using V5-tagged PCSK9 which disrupts its C-terminal phosphorylation could

affect any or all of these studies and thus could under represent a contribution of PCSK9 phosphorylation status in such studies.

4.4 Phosphorylation Modulates PCSK9 Function

PCSK9 and LDLR are both regulated co-directionally through the SREBP-2 pathway, even though PCSK9 post-translationally mediates LDLR degradation [49, 50]. It is possible that while PCSK9 is co-regulated transcriptionally with LDLR, another level of regulation at the post-translational level is present to fine tune its response to LDLR, perhaps mediated by PCSK9 phosphorylation status. Using SDM and transient transfection, we examined how different PCSK9 phosphomutants, those which prevented phosphorylation (phospho-null) and those which mimicked phosphorylation (phospho-mimick), affected corresponding LDLR protein levels. When phosphorylation was prevented at either site, LDLR levels increased significantly, while the double phosphonull mutant showed a non-significant increase in LDLR levels (Figure 13A and C). Based on our results, unphosphorylated PCSK9 shows less ability to degrade LDLR than phosphorylated forms of PCSK9.

We also substituted residues identified to be crucial to phosphorylation at both sites with aspartic acid or glutamic acid to determine whether simulating the size and/or charge of phosphoryl group addition could mimick the effect of phosphorylation on PCSK9 function. These acidic residues are commonly used to study phosphoproteins [135, 142, 143]. Glutamic acid in particular has been reported to provide a more valid simulation of phosphorylation [137]. When phosphorylation was mimicked by Glu in the N-terminus, a significant increase in LDLR degradation compared to hPCSK9(WT) was observed

supporting the notion that phosphorylation could provide additive 'gain of function' to PCSK9. Mimicking phosphorylation at the C-terminal site however did not result in a similar response, but instead LDLR levels were increased non-significantly. Both Phosphomimick double mutants PCSK9(S47D/S688D) and PCSK9(S47E/S688E) produced a similar response as observed with the C-terminal phosphomimick mutants. This suggested that substitution of Ser with Glu in PCSK9 propeptide was able to mimick phosphorylation at the N-terminus of PCSK9, but not in combination with, or at the C-terminal phosphorylation site alone.

In general, the C-terminal domains of PCSKs are implicated in protein-protein interaction [31] and specifically PCSK9 has been shown to interact with annexin A2 at unspecified residues within the C-terminal domain of PCSK9 [103]. Annexin A2 is reported to act as an endogenous inhibitor of PCSK9, by competitively binding to PCSK9 at the cell surface, sequestering it away from LDLR [103]. Since annexin A2 interacted with the C-terminus of PCSK9, we wanted to determine whether phosphorylation status of PCSK9 had an effect on this interaction. In our Far Western assay, we observed that spent media containing the doubly unphosphorylated hPCSK9(S47A/S688A) mutant bound to annexin A2 from HuH7 total cell lysates more strongly than phosphorylated hPCSK9(WT). In our functional assay mimicking phosphorylated PCSK9 promoted LDLR degradation while preventing PCSK9 phosphorylation reduced LDLR degradation suggesting a change in the interaction between PCSK9 and LDLR. Taking into account the results of the Far Western analysis, unphosphorylated PCSK9 more readily binds annexin A2, sequestering it at the cell surface away from LDLR, while phosphorylated PCSK9 remains free to bind LDLR and promote LDLR degradation leading to the 'gain of function' we observed. A similar effect was

previously described with respect to phosphorylation of the PCSK2 chaperone protein, 7B2 [122]. Phosphorylation of 7B2 reduced its binding affinity for PCSK2, which subsequently allowed for the activation of PCSK2.

4.5 Phosphorylation Provides Stability Against N-terminal Proteolysis

Phosphorylation status of a protein can affect its stability and half-life [119, 120]. While examining mass spectral plots of different PCSK9 mutants for differences in propeptide phosphorylation, we identified a propeptide fragment which appeared in hPCSK9(R46L)-V5 immunoprecipitates as well as in the engineered hPCSK9(E49A)-V5, but was not observed in hPCSK9(WT)-V5. This fragment corresponded to a proteolytic cleavage event occurring following the propeptide serine, Ser47 (Figure 14B). This propeptide cleavage product was also identified by ^{35}S-Met/Cys radiolabelling of immunoprecipitates of the propeptide hPCSK9(E49A)(Figure 14C). This suggested that phosphorylation at Ser47 in this region was protective and stabilizing for the PCSK9 propeptide. As well this cleavage product was visible, in the naturally occurring hPCSK9(R46L) variant which we demonstrated was significantly less phosphorylated in its propeptide (Figure 14A). The presence of a phosphoryl group can disrupt a protease recognition motif [135]. hPCSK9(R46L) is associated with hypocholesterolemia in humans, and several groups, including our group, have previously shown that individuals heterozygous for hPCSK9(R46L) have less circulating levels of PCSK9 than individuals with normal alleles [129, 136]. Could this proteolytic cleavage of hPCSK9(R46L) occur *in vivo*, and thus alter the half-life of PCSK9 resulting in the 'loss of function' phenotype observed with this variant? If so, this may begin to provide a mechanism through which hPCSK9(R46L) acts.

As mentioned earlier, phosphorylation status of PCSK9 affects its interaction with annexin A2. With regard to the availability of free circulating PCSK9 for interacting with and mediating LDLR degradation, phosphorylation status may contribute to PCSK9 availability by reducing the level of interaction with annexin A2 and promoting interaction with LDLR. Collectively these observations suggest that phosphorylation status modulates the half-life of PCSK9 propeptide, and availability of circulating PCSK9 in its phosphorylated form.

4.6 Proposed Mechanism For Phosphorylated PCSK9

Phosphorylation of PCSK9 is a functional modification which we have demonstrated can modulate its function and interactions. As a result we propose a modified mechanism of action for PCSK9 (Figure 17). PCSK9 is produced, matured through the secretory pathway, and secreted into circulation as a phosphoprotein. At the cell-surface phosphorylation status of PCSK9 determines a preferential interaction with LDLR (phosphorylated PCSK9) or annexin A2 (hypophosphorylated PCSK9). Unphosphorylated PCSK9 remains sequestered with annexin A2, functionally inactive, while phosphorylated PCSK9 interacts with LDLR, the complex enters the endocytic pathway and is redirected to the lysosome for degradation. Half-life of PCSK9 is affected to a degree by phosphorylation status of PCSK9 propeptide, as the hypophosphorylated form of the propeptide is more susceptible to proteolysis.

Figure 17. Proposed Mechanism Of Action for PCSK9. PCSK9 is constitutively secreted in several molecular forms (including phosphorylated and unphosphorylated). In the presence of annexin A2 at the cell surface, unphosphorylated PCSK9 preferentially interacts with and is sequestered at the cell surface by annexin A2, while phosphorylated PCSK9 will be available to bind to LDLR in the presence of annexin A2 and promote LDLR degradation. Unphosphorylated PCSK9 propeptide is more susceptible to proteolysis, potentially affecting the half-life of this molecular form versus phosphorylated PCSK9.

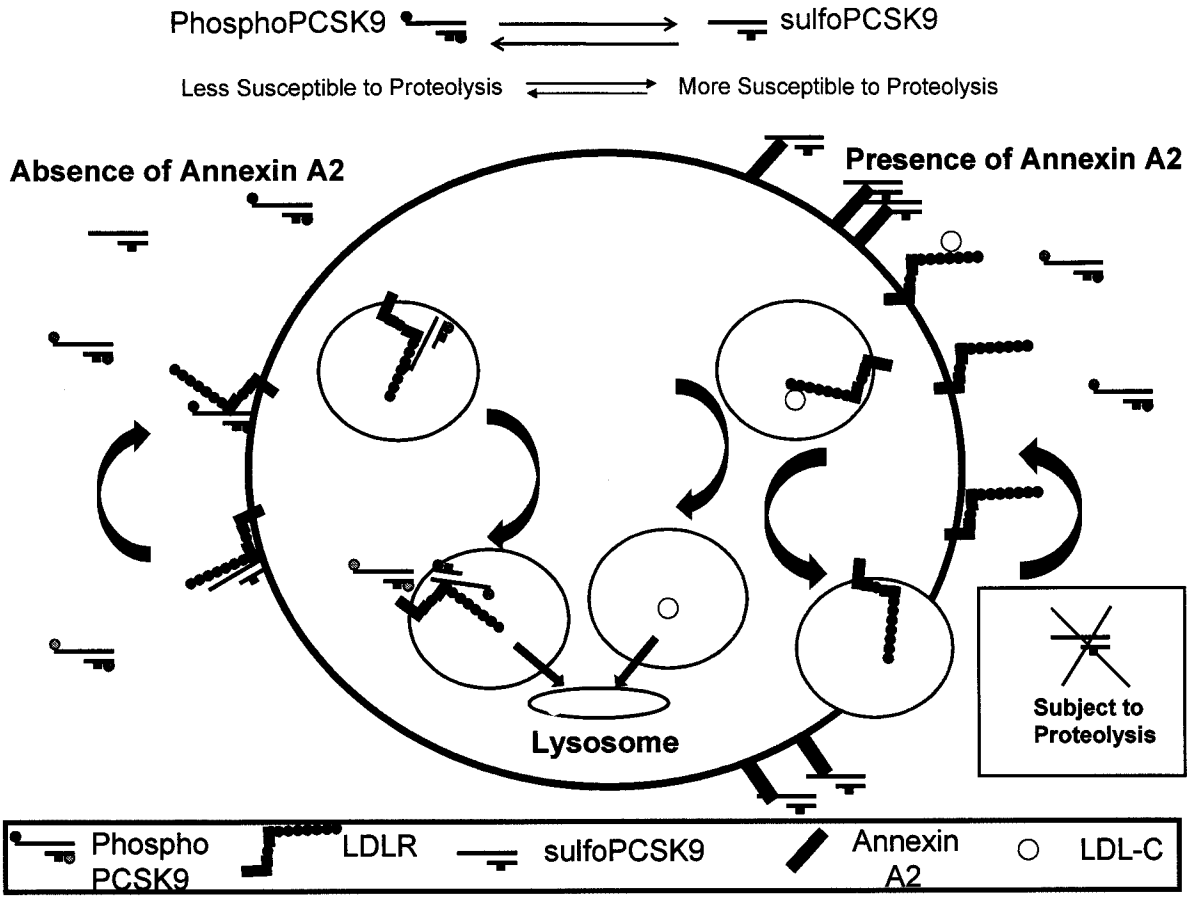
PhosphoPCSK9
sulfoPCSK9
Less Susceptible to Proteolysis
More Susceptible to Proteolysis
Absence of Annexin A2
Presence of Annexin A2
Lysosome
Subject to Proteolysis
Phospho PCSK9
LDLR
sulfoPCSK9
Annexin A2
LDL-C

5. Conclusion

More than 200 papers have been collectively published on PCSK9 in under a decade by groups from around the world, underscoring the interest in unraveling the mysteries of this convertase, in the pursuit of novel strategies for treating hypercholesterolemia and reducing the risk of developing heart disease. Many groups have attempted to shed light on the mechanisms governing PCSK9 mediated LDLR degradation. Here we demonstrated that PCSK9 is secreted as a phosphoprotein; PCSK9 is phosphorylated in its propeptide at Ser47, and in its C-terminal domain at Ser688. Using SDM we provided evidence that this functional post-translational modification affects PCSK9 propeptide stability, and PCSK9-mediated LDLR degradation; when phosphorylation of either phosphoserine was prevented, a significant recovery of LDLR levels was observed in cell culture. Phosphorylation of PCSK9 also reduced its interaction with an endogenous inhibitor, annexin A2.

6. References

1. Steiner, D.F. and P.E. Oyer, *The Biosynthesis of Insulin and a Probable Precursor of Insulin by a Human Islet Cell Adenoma.* Proc Natl Acad Sci U S A, 1967. **57**(2): p. 473-480.
2. Steiner, D.F., et al., *Insulin biosynthesis: evidence for a precursor.* Science, 1967. **157**(789): p. 697-700.
3. Chretien, M. and C.H. Li, *Isolation, purification, and characterization of gamma-lipotropic hormone from sheep pituitary glands.* Can J Biochem, 1967. **45**(7): p. 1163-74.
4. Julius, D., et al., *Isolation of the putative structural gene for the lysine-arginine-cleaving endopeptidase required for processing of yeast prepro-alpha-factor.* Cell, 1984. **37**(3): p. 1075-89.
5. Roebroek, A.J., et al., *Characterization of human c-fes/fps reveals a new transcription unit (fur) in the immediately upstream region of the proto-oncogene.* Mol Biol Rep, 1986. **11**(2): p. 117-25.
6. Seidah, N.G., et al., *cDNA sequence of two distinct pituitary proteins homologous to Kex2 and furin gene products: tissue-specific mRNAs encoding candidates for pro-hormone processing proteinases.* DNA Cell Biol, 1990. **9**(6): p. 415-24.
7. Nakagawa, T., et al., *Identification and functional expression of a new member of the mammalian Kex2-like processing endoprotease family: its striking structural similarity to PACE4.* J Biochem, 1993. **113**(2): p. 132-5.
8. Smeekens, S.P. and D.F. Steiner, *Identification of a human insulinoma cDNA encoding a novel mammalian protein structurally related to the yeast dibasic processing protease Kex2.* J Biol Chem, 1990. **265**(6): p. 2997-3000.
9. Nakayama, K., et al., *Identification of the fourth member of the mammalian endoprotease family homologous to the yeast Kex2 protease. Its testis-specific expression.* J Biol Chem, 1992. **267**(9): p. 5897-900.
10. Kiefer, M.C., et al., *Identification of a second human subtilisin-like protease gene in the fes/fps region of chromosome 15.* DNA Cell Biol, 1991. **10**(10): p. 757-69.
11. Munzer, J.S., et al., *In vitro characterization of the novel proprotein convertase PC7.* J Biol Chem, 1997. **272**(32): p. 19672-81.
12. Seidah, N.G., et al., *The secretory proprotein convertase neural apoptosis-regulated convertase 1 (NARC-1): liver regeneration and neuronal differentiation.* Proc Natl Acad Sci U S A, 2003. **100**(3): p. 928-33.
13. Seidah, N.G., et al., *The cDNA sequence of the human pro-hormone and pro-protein convertase PC1.* DNA Cell Biol, 1992. **11**(4): p. 283-9.
14. Seidah, N.G., et al., *cDNA structure, tissue distribution, and chromosomal localization of rat PC7, a novel mammalian proprotein convertase closest to yeast kexin-like proteinases.* Proc Natl Acad Sci U S A, 1996. **93**(8): p. 3388-93.
15. Smeekens, S.P., et al., *Identification of a cDNA encoding a second putative prohormone convertase related to PC2 in AtT20 cells and islets of Langerhans.* Proc Natl Acad Sci U S A, 1991. **88**(2): p. 340-4.
16. Constam, D.B., M. Calfon, and E.J. Robertson, *SPC4, SPC6, and the novel protease SPC7 are coexpressed with bone morphogenetic proteins at distinct sites during embryogenesis.* J Cell Biol, 1996. **134**(1): p. 181-91.

17. Lusson, J., et al., *cDNA structure of the mouse and rat subtilisin/kexin-like PC5: a candidate proprotein convertase expressed in endocrine and nonendocrine cells.* Proc Natl Acad Sci U S A, 1993. **90**(14): p. 6691-5.
18. Espenshade, P.J., et al., *Autocatalytic processing of site-1 protease removes propeptide and permits cleavage of sterol regulatory element-binding proteins.* J Biol Chem, 1999. **274**(32): p. 22795-804.
19. Seidah, N.G., et al., *Mammalian subtilisin/kexin isozyme SKI-1: A widely expressed proprotein convertase with a unique cleavage specificity and cellular localization.* Proc Natl Acad Sci U S A, 1999. **96**(4): p. 1321-6.
20. Shennan, K.I., et al., *Characterization of PC2, a mammalian Kex2 homologue, following expression of the cDNA in microinjected Xenopus oocytes.* FEBS Lett, 1991. **284**(2): p. 277-80.
21. Seidah, N.G., et al., *The subtilisin/kexin family of precursor convertases. Emphasis on PC1, PC2/7B2, POMC and the novel enzyme SKI-1.* Ann N Y Acad Sci, 1999. **885**: p. 57-74.
22. Rouille, Y., et al., *Proglucagon is processed to glucagon by prohormone convertase PC2 in alpha TC1-6 cells.* Proc Natl Acad Sci U S A, 1994. **91**(8): p. 3242-6.
23. Bravo, D.A., et al., *Accurate and efficient cleavage of the human insulin proreceptor by the human proprotein-processing protease furin. Characterization and kinetic parameters using the purified, secreted soluble protease expressed by a recombinant baculovirus.* J Biol Chem, 1994. **269**(41): p. 25830-7.
24. Duguay, S.J., et al., *Processing of wild-type and mutant proinsulin-like growth factor-IA by subtilisin-related proprotein convertases.* J Biol Chem, 1997. **272**(10): p. 6663-70.
25. Valore, E.V. and T. Ganz, *Posttranslational processing of hepcidin in human hepatocytes is mediated by the prohormone convertase furin.* Blood Cells Mol Dis, 2008. **40**(1): p. 132-8.
26. Bergeron, E., et al., *Processing of alpha4 integrin by the proprotein convertases: histidine at position P6 regulates cleavage.* Biochem J, 2003. **373**(Pt 2): p. 475-84.
27. Rholam, M. and C. Fahy, *Processing of peptide and hormone precursors at the dibasic cleavage sites.* Cell Mol Life Sci, 2009. **66**(13): p. 2075-91.
28. Seidah, N.G. and A. Prat, *The proprotein convertases are potential targets in the treatment of dyslipidemia.* J Mol Med, 2007. **85**(7): p. 685-96.
29. Seidah, N.G., M. Chretien, and R. Day, *The family of subtilisin/kexin like pro-protein and pro-hormone convertases: divergent or shared functions.* Biochimie, 1994. **76**(3-4): p. 197-209.
30. Muller, L. and I. Lindberg, *The cell biology of the prohormone convertases PC1 and PC2.* Prog Nucleic Acid Res Mol Biol, 1999. **63**: p. 69-108.
31. Seidah, N.G. and A. Prat, *Precursor convertases in the secretory pathway, cytosol and extracellular milieu.* Essays Biochem, 2002. **38**: p. 79-94.
32. Benjannet, S., et al., *NARC-1/PCSK9 and its natural mutants: zymogen cleavage and effects on the low density lipoprotein (LDL) receptor and LDL cholesterol.* J Biol Chem, 2004. **279**(47): p. 48865-75.
33. van de Ven, W.J., et al., *Furin is a subtilisin-like proprotein processing enzyme in higher eukaryotes.* Mol Biol Rep, 1990. **14**(4): p. 265-75.

34. Hosaka, M., et al., *Arg-X-Lys/Arg-Arg motif as a signal for precursor cleavage catalyzed by furin within the constitutive secretory pathway.* J Biol Chem, 1991. **266**(19): p. 12127-30.
35. Zhong, M., et al., *Functional analysis of human PACE4-A and PACE4-C isoforms: identification of a new PACE4-CS isoform.* FEBS Lett, 1996. **396**(1): p. 31-6.
36. van de Loo, J.W., et al., *Biosynthesis, distinct post-translational modifications, and functional characterization of lymphoma proprotein convertase.* J Biol Chem, 1997. **272**(43): p. 27116-23.
37. De Bie, I., et al., *The isoforms of proprotein convertase PC5 are sorted to different subcellular compartments.* J Cell Biol, 1996. **135**(5): p. 1261-75.
38. Li, M., M. Mbikay, and A. Arimura, *Pituitary adenylate cyclase-activating polypeptide precursor is processed solely by prohormone convertase 4 in the gonads.* Endocrinology, 2000. **141**(10): p. 3723-30.
39. Molloy, S.S., et al., *Intracellular trafficking and activation of the furin proprotein convertase: localization to the TGN and recycling from the cell surface.* Embo J, 1994. **13**(1): p. 18-33.
40. Zhu, X., et al., *Disruption of PC1/3 expression in mice causes dwarfism and multiple neuroendocrine peptide processing defects.* Proc Natl Acad Sci U S A, 2002. **99**(16): p. 10293-8.
41. Furuta, M., et al., *Defective prohormone processing and altered pancreatic islet morphology in mice lacking active SPC2.* Proc Natl Acad Sci U S A, 1997. **94**(13): p. 6646-51.
42. Roebroek, A.J., et al., *Failure of ventral closure and axial rotation in embryos lacking the proprotein convertase Furin.* Development, 1998. **125**(24): p. 4863-76.
43. Mbikay, M., et al., *Impaired fertility in mice deficient for the testicular germ-cell protease PC4.* Proc Natl Acad Sci U S A, 1997. **94**(13): p. 6842-6.
44. Essalmani, R., et al., *Deletion of the gene encoding proprotein convertase 5/6 causes early embryonic lethality in the mouse.* Mol Cell Biol, 2006. **26**(1): p. 354-61.
45. Constam, D.B. and E.J. Robertson, *SPC4/PACE4 regulates a TGFbeta signaling network during axis formation.* Genes Dev, 2000. **14**(9): p. 1146-55.
46. Yang, J., et al., *Decreased lipid synthesis in livers of mice with disrupted Site-1 protease gene.* Proc Natl Acad Sci U S A, 2001. **98**(24): p. 13607-12.
47. Rashid, S., et al., *Decreased plasma cholesterol and hypersensitivity to statins in mice lacking Pcsk9.* Proc Natl Acad Sci U S A, 2005. **102**(15): p. 5374-9.
48. Siegfried, G., et al., *Regulation of the stepwise proteolytic cleavage and secretion of PDGF-B by the proprotein convertases.* Oncogene, 2005. **24**(46): p. 6925-35.
49. Park, S.W., Y.A. Moon, and J.D. Horton, *Post-transcriptional regulation of low density lipoprotein receptor protein by proprotein convertase subtilisin/kexin type 9a in mouse liver.* J Biol Chem, 2004. **279**(48): p. 50630-8.
50. Maxwell, K.N. and J.L. Breslow, *Adenoviral-mediated expression of Pcsk9 in mice results in a low-density lipoprotein receptor knockout phenotype.* Proc Natl Acad Sci U S A, 2004. **101**(18): p. 7100-5.
51. Cohen, J., et al., *Low LDL cholesterol in individuals of African descent resulting from frequent nonsense mutations in PCSK9.* Nat Genet, 2005. **37**(2): p. 161-5.
52. Cohen, J.C., et al., *Sequence variations in PCSK9, low LDL, and protection against coronary heart disease.* N Engl J Med, 2006. **354**(12): p. 1264-72.

53. Hooper, A.J., et al., *The C679X mutation in PCSK9 is present and lowers blood cholesterol in a Southern African population.* Atherosclerosis, 2007. **193**(2): p. 445-8.
54. Zhao, Z., et al., *Molecular characterization of loss-of-function mutations in PCSK9 and identification of a compound heterozygote.* Am J Hum Genet, 2006. **79**(3): p. 514-23.
55. Izem, L., et al., *Effect of reduced low-density lipoprotein receptor level on HepG2 cell cholesterol metabolism.* Biochem J, 1998. **329 (Pt 1)**: p. 81-9.
56. Brown, M.S. and J.L. Goldstein, *A receptor-mediated pathway for cholesterol homeostasis.* Science, 1986. **232**(4746): p. 34-47.
57. Kane, J.P., *Apolipoprotein B: structural and metabolic heterogeneity.* Annu Rev Physiol, 1983. **45**: p. 637-50.
58. Marcel, Y.L., et al., *Mapping of human apolipoprotein B antigenic determinants.* Arteriosclerosis, 1987. **7**(2): p. 166-75.
59. Garcia, C.K., et al., *Autosomal recessive hypercholesterolemia caused by mutations in a putative LDL receptor adaptor protein.* Science, 2001. **292**(5520): p. 1394-8.
60. He, G., et al., *ARH is a modular adaptor protein that interacts with the LDL receptor, clathrin, and AP-2.* J Biol Chem, 2002. **277**(46): p. 44044-9.
61. Sirinian, M.I., et al., *Adaptor protein ARH is recruited to the plasma membrane by low density lipoprotein (LDL) binding and modulates endocytosis of the LDL/LDL receptor complex in hepatocytes.* J Biol Chem, 2005. **280**(46): p. 38416-23.
62. Zhang, D.W., et al., *Structural requirements for PCSK9-mediated degradation of the low-density lipoprotein receptor.* Proc Natl Acad Sci U S A, 2008. **105**(35): p. 13045-50.
63. Davis, C.G., et al., *Acid-dependent ligand dissociation and recycling of LDL receptor mediated by growth factor homology region.* Nature, 1987. **326**(6115): p. 760-5.
64. Abifadel, M., et al., *Mutations and polymorphisms in the proprotein convertase subtilisin kexin 9 (PCSK9) gene in cholesterol metabolism and disease.* Hum Mutat, 2009. **30**(4): p. 520-9.
65. Khachadurian, A.K., *The Inheritance of Essential Familial Hypercholesterolemia.* Am J Med, 1964. **37**: p. 402-7.
66. Abifadel, M., et al., *Mutations in PCSK9 cause autosomal dominant hypercholesterolemia.* Nat Genet, 2003. **34**(2): p. 154-6.
67. Brown, M.S. and J.L. Goldstein, *Familial hypercholesterolemia: defective binding of lipoproteins to cultured fibroblasts associated with impaired regulation of 3-hydroxy-3-methylglutaryl coenzyme A reductase activity.* Proc Natl Acad Sci U S A, 1974. **71**(3): p. 788-92.
68. Innerarity, T.L., et al., *Familial defective apolipoprotein B-100: a mutation of apolipoprotein B that causes hypercholesterolemia.* J Lipid Res, 1990. **31**(8): p. 1337-49.
69. Innerarity, T.L., et al., *Familial defective apolipoprotein B-100: low density lipoproteins with abnormal receptor binding.* Proc Natl Acad Sci U S A, 1987. **84**(19): p. 6919-23.
70. Goldstein, J.L., et al., *Genetic heterogeneity in familial hypercholesterolemia: evidence for two different mutations affecting functions of low-density lipoprotein receptor.* Proc Natl Acad Sci U S A, 1975. **72**(3): p. 1092-6.

71. Brown, M.S. and J.L. Goldstein, *Human mutations affecting the low density lipoprotein pathway.* Am J Clin Nutr, 1977. **30**(6): p. 975-8.
72. Francke, U., M.S. Brown, and J.L. Goldstein, *Assignment of the human gene for the low density lipoprotein receptor to chromosome 19: synteny of a receptor, a ligand, and a genetic disease.* Proc Natl Acad Sci U S A, 1984. **81**(9): p. 2826-30.
73. Stenson, P.D., et al., *Human Gene Mutation Database (HGMD): 2003 update.* Hum Mutat, 2003. **21**(6): p. 577-81.
74. Grundy, S.M., G.L. Vega, and Y.A. Kesaniemi, *Abnormalities in metabolism of low density lipoproteins associated with coronary heart disease.* Acta Med Scand Suppl, 1985. **701**: p. 23-37.
75. Varret, M., et al., *A third major locus for autosomal dominant hypercholesterolemia maps to 1p34.1-p32.* Am J Hum Genet, 1999. **64**(5): p. 1378-87.
76. Timms, K.M., et al., *A mutation in PCSK9 causing autosomal-dominant hypercholesterolemia in a Utah pedigree.* Hum Genet, 2004. **114**(4): p. 349-53.
77. Blesa, S., et al., *A New PCSK9 Gene Promoter Variant Affects Gene Expression and Causes Autosomal Dominant Hypercholesterolemia.* J Clin Endocrinol Metab, 2008. **93**(9): p. 3577-83.
78. Cameron, J., et al., *Characterization of novel mutations in the catalytic domain of the PCSK9 gene.* J Intern Med, 2008. **263**(4): p. 420-31.
79. Costet, P., et al., *Hepatic PCSK9 expression is regulated by nutritional status via insulin and sterol regulatory element-binding protein 1c.* J Biol Chem, 2006. **281**(10): p. 6211-8.
80. Dubuc, G., et al., *Statins upregulate PCSK9, the gene encoding the proprotein convertase neural apoptosis-regulated convertase-1 implicated in familial hypercholesterolemia.* Arterioscler Thromb Vasc Biol, 2004. **24**(8): p. 1454-9.
81. Li, H., et al., *HNF1{alpha} plays a critical role in PCSK9 gene transcription and regulation by a natural hypocholesterolemic compound berberine.* J Biol Chem, 2009.
82. Yokoyama, C., et al., *SREBP-1, a basic-helix-loop-helix-leucine zipper protein that controls transcription of the low density lipoprotein receptor gene.* Cell, 1993. **75**(1): p. 187-97.
83. Hua, X., et al., *SREBP-2, a second basic-helix-loop-helix-leucine zipper protein that stimulates transcription by binding to a sterol regulatory element.* Proc Natl Acad Sci U S A, 1993. **90**(24): p. 11603-7.
84. Lopez, J.M., et al., *Sterol regulation of acetyl coenzyme A carboxylase: a mechanism for coordinate control of cellular lipid.* Proc Natl Acad Sci U S A, 1996. **93**(3): p. 1049-53.
85. Kawabe, Y., et al., *The physiological role of sterol regulatory element-binding protein-2 in cultured human cells.* Biochim Biophys Acta, 1999. **1436**(3): p. 307-18.
86. Mayne, J., et al., *Plasma PCSK9 levels are significantly modified by statins and fibrates in humans.* Lipids Health Dis, 2008. **7**: p. 22.
87. Persson, L., et al., *Importance of proprotein convertase subtilisin/kexin type 9 in the hormonal and dietary regulation of rat liver low-density lipoprotein receptors.* Endocrinology, 2009. **150**(3): p. 1140-6.
88. Langhi, C., et al., *Activation of the farnesoid X receptor represses PCSK9 expression in human hepatocytes.* FEBS Lett, 2008. **582**(6): p. 949-55.

89. Benjannet, S., et al., *The proprotein convertase (PC) PCSK9 is inactivated by furin and/or PC5/6A: functional consequences of natural mutations and post-translational modifications.* J Biol Chem, 2006. **281**(41): p. 30561-72.
90. Dewpura, T., et al., *PCSK9 is phosphorylated by a Golgi casein kinase-like kinase ex vivo and circulates as a phosphoprotein in humans.* FEBS J, 2008. **275**(13): p. 3480-93.
91. Cameron, J., et al., *Effect of mutations in the PCSK9 gene on the cell surface LDL receptors.* Hum Mol Genet, 2006. **15**(9): p. 1551-8.
92. Lagace, T.A., et al., *Secreted PCSK9 decreases the number of LDL receptors in hepatocytes and in livers of parabiotic mice.* J Clin Invest, 2006. **116**(11): p. 2995-3005.
93. McNutt, M.C., T.A. Lagace, and J.D. Horton, *Catalytic activity is not required for secreted PCSK9 to reduce low density lipoprotein receptors in HepG2 cells.* J Biol Chem, 2007. **282**(29): p. 20799-803.
94. Grefhorst, A., et al., *Plasma PCSK9 preferentially reduces liver LDL receptors in mice.* J Lipid Res, 2008. **49**(6): p. 1303-11.
95. Zhang, D.W., et al., *Binding of proprotein convertase subtilisin/kexin type 9 to epidermal growth factor-like repeat A of low density lipoprotein receptor decreases receptor recycling and increases degradation.* J Biol Chem, 2007. **282**(25): p. 18602-12.
96. Kwon, H.J., et al., *Molecular basis for LDL receptor recognition by PCSK9.* Proc Natl Acad Sci U S A, 2008. **105**(6): p. 1820-5.
97. McNutt, M.C., et al., *Antagonism of secreted PCSK9 increases low density lipoprotein receptor expression in HepG2 cells.* J Biol Chem, 2009. **284**(16): p. 10561-70.
98. Cunningham, D., et al., *Structural and biophysical studies of PCSK9 and its mutants linked to familial hypercholesterolemia.* Nat Struct Mol Biol, 2007. **14**(5): p. 413-9.
99. Maxwell, K.N., E.A. Fisher, and J.L. Breslow, *Overexpression of PCSK9 accelerates the degradation of the LDLR in a post-endoplasmic reticulum compartment.* Proc Natl Acad Sci U S A, 2005. **102**(6): p. 2069-74.
100. Poirier, S., et al., *Dissection of the endogenous cellular pathways of PCSK9-induced low density lipoprotein receptor degradation: evidence for an intracellular route.* J Biol Chem, 2009. **284**(42): p. 28856-64.
101. Shan, L., et al., *PCSK9 binds to multiple receptors and can be functionally inhibited by an EGF-A peptide.* Biochem Biophys Res Commun, 2008. **375**(1): p. 69-73.
102. Chan, J.C., et al., *A proprotein convertase subtilisin/kexin type 9 neutralizing antibody reduces serum cholesterol in mice and nonhuman primates.* Proc Natl Acad Sci U S A, 2009. **106**(24): p. 9820-5.
103. Mayer, G., S. Poirier, and N.G. Seidah, *Annexin A2 is a C-terminal PCSK9-binding protein that regulates endogenous low density lipoprotein receptor levels.* J Biol Chem, 2008. **283**(46): p. 31791-801.
104. Choi, K.S., et al., *Annexin II tetramer inhibits plasmin-dependent fibrinolysis.* Biochemistry, 1998. **37**(2): p. 648-55.
105. Hajjar, K.A. and S.S. Acharya, *Annexin II and regulation of cell surface fibrinolysis.* Ann N Y Acad Sci, 2000. **902**: p. 265-71.
106. Hajjar, K.A. and S. Krishnan, *Annexin II: a mediator of the plasmin/plasminogen activator system.* Trends Cardiovasc Med, 1999. **9**(5): p. 128-38.

107. Morel, E. and J. Gruenberg, *Annexin A2 binding to endosomes and functions in endosomal transport are regulated by tyrosine 23 phosphorylation.* J Biol Chem, 2009. **284**(3): p. 1604-11.
108. Hajjar, K.A., et al., *Interaction of the fibrinolytic receptor, annexin II, with the endothelial cell surface. Essential role of endonexin repeat 2.* J Biol Chem, 1996. **271**(35): p. 21652-9.
109. Rety, S., et al., *The crystal structure of a complex of p11 with the annexin II N-terminal peptide.* Nat Struct Biol, 1999. **6**(1): p. 89-95.
110. Luo, Y., et al., *Function and distribution of circulating human PCSK9 expressed extrahepatically in transgenic mice.* J Lipid Res, 2009. **50**(8): p. 1581-8.
111. Hammarsten, *Zur Frage, ob das Casein ein einheitlicher Stoff sei.* Z. Physiol. Chem., 1883. **7**: p. 227- 273.
112. Burnett, G. and E.P. Kennedy, *The enzymatic phosphorylation of proteins.* J Biol Chem, 1954. **211**(2): p. 969-80.
113. Long, C., *The hexokinase activity of rat tissues.* Biochem J, 1951. **49**(3): p. xxxiv-xxxv.
114. Eckhart, W., M.A. Hutchinson, and T. Hunter, *An activity phosphorylating tyrosine in polyoma T antigen immunoprecipitates.* Cell, 1979. **18**(4): p. 925-33.
115. Khomutov, R.M., et al., *Phosphorylation of threonine residue in apo-aspartate aminotransferase during the inhibition with N-(pyridoxyl-5'-phosphate)-L-glutamic acid.* Biochim Biophys Acta, 1969. **171**(1): p. 201-2.
116. Olsen, J.V., et al., *Global, in vivo, and site-specific phosphorylation dynamics in signaling networks.* Cell, 2006. **127**(3): p. 635-48.
117. Hefner, Y., et al., *Serine 727 phosphorylation and activation of cytosolic phospholipase A2 by MNK1-related protein kinases.* J Biol Chem, 2000. **275**(48): p. 37542-51.
118. Russo, A.A., P.D. Jeffrey, and N.P. Pavletich, *Structural basis of cyclin-dependent kinase activation by phosphorylation.* Nat Struct Biol, 1996. **3**(8): p. 696-700.
119. Winston, J.T., et al., *The SCFbeta-TRCP-ubiquitin ligase complex associates specifically with phosphorylated destruction motifs in IkappaBalpha and beta-catenin and stimulates IkappaBalpha ubiquitination in vitro.* Genes Dev, 1999. **13**(3): p. 270-83.
120. Liu, C., et al., *Control of beta-catenin phosphorylation/degradation by a dual-kinase mechanism.* Cell, 2002. **108**(6): p. 837-47.
121. Takahashi, S., et al., *Localization of furin to the trans-Golgi network and recycling from the cell surface involves Ser and Tyr residues within the cytoplasmic domain.* J Biol Chem, 1995. **270**(47): p. 28397-401.
122. Lee, S.N., J.R. Hwang, and I. Lindberg, *Neuroendocrine protein 7B2 can be inactivated by phosphorylation within the secretory pathway.* J Biol Chem, 2006. **281**(6): p. 3312-20.
123. Manning, G., et al., *The protein kinase complement of the human genome.* Science, 2002. **298**(5600): p. 1912-34.
124. Procino, G., et al., *Ser-256 phosphorylation dynamics of Aquaporin 2 during maturation from the ER to the vesicular compartment in renal cells.* Faseb J, 2003. **17**(13): p. 1886-8.
125. Lasa, M., et al., *Phosphorylation of osteopontin by Golgi apparatus casein kinase.* Biochem Biophys Res Commun, 1997. **240**(3): p. 602-5.

126. Jones, B.G., et al., *Intracellular trafficking of furin is modulated by the phosphorylation state of a casein kinase II site in its cytoplasmic tail.* Embo J, 1995. **14**(23): p. 5869-83.
127. Coverley, J.A., J.L. Martin, and R.C. Baxter, *The effect of phosphorylation by casein kinase 2 on the activity of insulin-like growth factor-binding protein-3.* Endocrinology, 2000. **141**(2): p. 564-70.
128. Jones, J.I., et al., *Phosphorylation of insulin-like growth factor (IGF)-binding protein 1 in cell culture and in vivo: effects on affinity for IGF-I.* Proc Natl Acad Sci U S A, 1991. **88**(17): p. 7481-5.
129. Mayne, J., et al., *Plasma PCSK9 levels correlate with cholesterol in men but not in women.* Biochem Biophys Res Commun, 2007. **361**(2): p. 451-6.
130. Craig, A.G., et al., *Monitoring protein kinase and phosphatase reactions with matrix-assisted laser desorption/ionization mass spectrometry and capillary zone electrophoresis: comparison of the detection efficiency of peptide-phosphopeptide mixtures.* Biol Mass Spectrom, 1994. **23**(8): p. 519-28.
131. Kuenzel, E.A., et al., *Substrate specificity determinants for casein kinase II as deduced from studies with synthetic peptides.* J Biol Chem, 1987. **262**(19): p. 9136-40.
132. Marin, O., et al., *Site specificity of casein kinase-2 (TS) from rat liver cytosol. A study with model peptide substrates.* Eur J Biochem, 1986. **160**(2): p. 239-44.
133. Brunati, A.M., et al., *Novel consensus sequence for the Golgi apparatus casein kinase, revealed using proline-rich protein-1 (PRP1)-derived peptide substrates.* Biochem J, 2000. **351 Pt 3**: p. 765-8.
134. Lasa-Benito, M., et al., *Golgi apparatus mammary gland casein kinase: monitoring by a specific peptide substrate and definition of specificity determinants.* FEBS Lett, 1996. **382**(1-2): p. 149-52.
135. Littlepage, L.E., et al., *Identification of phosphorylated residues that affect the activity of the mitotic kinase Aurora-A.* Proc Natl Acad Sci U S A, 2002. **99**(24): p. 15440-5.
136. Strom, T.B., et al., *Loss-of-function mutation R46L in the PCSK9 gene has little impact on the levels of total serum cholesterol in familial hypercholesterolemia heterozygotes.* Clin Chim Acta, 2009.
137. Anthis, N.J., et al., *Beta integrin tyrosine phosphorylation is a conserved mechanism for regulating talin-induced integrin activation.* J Biol Chem, 2009. **284**(52): p. 36700-10.
138. Ding, K., S.J. McDonough, and I.J. Kullo, *Evidence for positive selection in the C-terminal domain of the cholesterol metabolism gene PCSK9 based on phylogenetic analysis in 14 primate species.* PLoS ONE, 2007. **2**(10): p. e1098.
139. Tibaldi, E., et al., *Analysis of a sub-proteome which co-purifies with and is phosphorylated by the Golgi casein kinase.* Cell Mol Life Sci, 2006. **63**(3): p. 378-89.
140. Lasa, M., O. Marin, and L.A. Pinna, *Rat liver Golgi apparatus contains a protein kinase similar to the casein kinase of lactating mammary gland.* Eur J Biochem, 1997. **243**(3): p. 719-25.
141. Hampton, E.N., et al., *The self-inhibited structure of full-length PCSK9 at 1.9 A reveals structural homology with resistin within the C-terminal domain.* Proc Natl Acad Sci U S A, 2007. **104**(37): p. 14604-9.

142. Burkart, E.M., et al., *Phosphorylation or glutamic acid substitution at protein kinase C sites on cardiac troponin I differentially depress myofilament tension and shortening velocity.* J Biol Chem, 2003. **278**(13): p. 11265-72.
143. Brown, N.M., et al., *Novel role of phosphorylation in Fe-S cluster stability revealed by phosphomimetic mutations at Ser-138 of iron regulatory protein 1.* Proc Natl Acad Sci U S A, 1998. **95**(26): p. 15235-40.